






Cite this: *Sustainable Energy Fuels*,  
2024, 8, 379

## Valorisation of residual biomass by pyrolysis: influence of process conditions on products

A. C. M. Vilas-Boas,  L. A. C. Tarelho, \* H. S. M. Oliveira, F. G. C. S. Silva, D. T. Pio   
and M. A. A. Matos

In the context of sustainable residual biomass management, this work explores the pyrolysis process of residual biomass using a bench-scale fixed bed reactor. The main focus is to comprehensively analyze the effects of diverse forest and agroforestry biomass, pyrolysis temperature (350, 450 and 550 °C) and heating rate (2, 10 and 30 °C min<sup>-1</sup>) on the yield of the products biochar, bio-oil and permanent gas, and on the composition of biochar and permanent gas. This analysis provides a valuable collection of insights to support the advancement of pyrolysis projects and their expansion into industrial production, facilitating the creation of versatile products. The study showed that the biochar, bio-oil and permanent gas yields were between 0.22 and 0.47, 0.26 and 0.59 and 0.17 and 0.41 kg kg<sup>-1</sup> dry biomass, respectively. The pyrolysis of olive pomace has the maximum biochar yield, that of eucalyptus sawdust has the maximum bio-oil yield, and that of giant reed has the maximum permanent gas yield. The increased temperature led to a decreased biochar yield and an increased bio-oil yield. The increased heating rate led to a decreased biochar yield and an increased bio-oil yield. Biochar has a carbon content above 0.7 kg kg<sup>-1</sup> dry ash free, with an LHV between 24.2 and 30.5 MJ kg<sup>-1</sup> dry biochar, suggesting potential for soil enrichment and the energy vector. Permanent gas has an LHV between 5.4 and 9.7 MJ Nm<sup>-3</sup>, and seems useful as a thermal energy source to support the pyrolysis process.

Received 16th September 2023  
Accepted 1st December 2023

DOI: 10.1039/d3se01216f

rsc.li/sustainable-energy

### 1. Introduction

There has been a rapid global growth of interest in diverse renewable energy sources for decarbonizing the society.<sup>1</sup> Biomass, including agricultural wastes and forestry residues is considered a promising competitive candidate for replacing fossil fuel production and supply.<sup>2–4</sup> Therefore, thermochemical conversion of biomass into biofuels and other value added and environment friendly compounds has attracted substantial research attention.<sup>5</sup>

Thermochemical conversion of biomass concerns all processes characterized by higher temperature to convert biomass into more useful product streams.<sup>2,3,5</sup> Pyrolysis is one of these process, in which the thermo-chemical conversion of biomass is performed in the absence of oxygen.<sup>3,4,6</sup> During pyrolysis, the biomass structure is thermally broken down into char (solid fraction), bio-oil (condensed vapors) and permanent gas (non-condensable gases under atmospheric conditions). The relative amount and composition of these products depend on several factors, including the pyrolysis heating rate, temperature, residence time, technology, and biomass characteristics.<sup>7</sup>

This process involves different overlapping stages: drying and primary and secondary reactions.<sup>7–9</sup> These reactions are mostly endothermic. First, during heating of the solid fuel particle, water is evaporated (drying stage, which usually occurs until around 100 °C) and then a progressive release of volatiles occurs with temperature increase (primary pyrolysis stage, until approximately 500 °C). This release of volatiles is the main stage of the pyrolysis process, where large molecules of the organic matrix of biomass particles decompose into primary volatiles (condensable gases and permanent gases) and primary char, accompanied by a significant weight loss of the original solid biomass particle.<sup>7–9</sup> If the biomass is further converted at higher temperatures, some of the primary volatiles released into the particle can participate in a variety of secondary reactions. The primary and secondary reactions can take place simultaneously on different parts of a biomass particle.<sup>8</sup> The composition of volatiles is a combined effect of primary and secondary pyrolysis conversion.<sup>7,8</sup>

Biomass mainly consists of three macro-components: cellulose (30–60%), hemicellulose (20–35%) and lignin (15–30%), that decompose in different temperature ranges during thermochemical conversion of biomass.<sup>10</sup> These main macro-components of biomass undergo pyrolysis in distinct ways, thus contributing differently to the yields of the pyrolysis products. For example, cellulose and hemicellulose are the main sources of volatile matter in lignocellulosic biomass.

Department of Environment and Planning & Centre for Environmental and Marine Studies (CESAM), University of Aveiro, Aveiro, Portugal. E-mail: ltarelho@ua.pt



Cellulose is a primary source of condensable vapors, whereas hemicellulose contributes more to the production of non-condensable vapors.<sup>11</sup> Lignin decomposes slowly, making a major contribution to the char yield, due to its aromatic content.<sup>7</sup> Additionally, the particle size, shape, and physical structure of the biomass influence the pyrolytic products by affecting heat and mass transfer throughout the process. Finer particles provide less resistance to the release of condensable vapors, which therefore escape relatively easily to the surroundings before undergoing secondary cracking, resulting in a higher bio-oil yield.<sup>7</sup>

Char is mainly composed of carbon, but it also contains oxygen, hydrogen and inorganic elements (ash). The lower heating value (LHV) of char is between 22 and 34 MJ kg<sup>-1</sup> dry basis,<sup>7,12–14</sup> which is substantially higher than that of the raw biomass, between 15 and 20 MJ kg<sup>-1</sup> dry basis.<sup>8,15–17</sup> Bio-oil consists of water and a complex mix of oxygenated organic compounds, such as aldehydes, ketones, acids, alcohols, sugars and dehydrosugars and phenolic compounds.<sup>7,18–20</sup> The permanent gas (not condensable vapors) is composed of the following most relevant components CO<sub>2</sub>, CO, H<sub>2</sub>, CH<sub>4</sub>, and other light hydrocarbons (C<sub>x</sub>H<sub>y</sub>) and has a LHV ranging from 3 to 15 MJ Nm<sup>-3</sup>.<sup>7,13,19,21</sup>

Based on the heating rate imposed on the biomass particles, pyrolysis may be classified into two main categories of processes: fast or slow. Fast pyrolysis is characterized by a high heating rate (e.g., 100 to 1000 °C s<sup>-1</sup>) and a very short residence time in the gas phase (below 1 s), resulting in the production of bio-oil with yields between 65 and 75 %wt. and char with yields between 10 and 30 %wt.<sup>6,22,23</sup> The bio-oil is considered a versatile raw material that can be refined or processed in different ways to meet various needs, including the production of transportation fuels and chemicals with added value. The char and permanent gas can be used as fuel to provide thermal energy for the pyrolysis process or for heat and power generation.<sup>3,23</sup> Slow pyrolysis is characterized by low heating rates (e.g., <1 °C s<sup>-1</sup>) and a long residence time in the solid phase (between minutes and days),<sup>7,24,25</sup> and produces char with yields between 25 and 35 %wt. and bio-oil with yields between 20 and 50 %wt.<sup>6</sup> The char applications typically involve water treatment, energy generation, soil amendment, and carbon sink, among other applications.<sup>6,26–28</sup>

Pyrolysis of residual biomass has been studied and developed for different purposes. For example, Yang *et al.*<sup>29</sup> studied the production of bio-oil to mix with diesel. Bio-oil was produced by fast pyrolysis of coffee bean residue, and it was found that the high-water content in bio-oil causes a reduction in its heating value, but the authors observed that the emulsification properties of the fuel mixture bio-oil/diesel enhanced certain aspects of combustion, with NO<sub>x</sub> emission reduction in certain proportions of bio-oil. Zhou *et al.*<sup>30</sup> studied co-application of biochar and bio-oil for valorization as an asphalt material, and found that biochar can remarkably modify the performance of petroleum asphalt, including penetration, softening point, ductility, viscosity and complex modulus, and that the upgraded bio-oil can be used to partly or fully replace petroleum asphalt, which is a promising biomass

application. Liang *et al.*<sup>26</sup> studied the biochar application as a soil amendment, and found that biochar application in alkaline saline soil improved the physical and hydraulic properties of saline-alkaline soil (e.g., increased soil porosity and decreased the bulk density).

However, most of the studies on the pyrolysis of biomass rely on a specific biomass type and on the yield and characteristics of a specific product or application, and mostly on biochar and bio-oil.<sup>31–34</sup> In fact, it is recognized that a more comprehensive approach is needed, involving the integrated analysis of pyrolysis experiments using different types of residual biomass, including the analysis of the distribution and characteristics of the resulting products, biochar, bio-oil and gas, and the influence of process conditions such as the temperature and heating rate, to drive the development of pyrolysis projects and their expansion into industrial production.

In this context, this study adopts a new approach by simultaneously conducting an experimental analysis under different pyrolysis conditions, specifically involving distinct types of residual forestry and agroforestry biomass, and different temperatures, and heating rates. This is supplemented by a comprehensive characterization of biochar and gases. The pyrolysis experiments were performed in a bench-scale fixed bed reactor.

Remarkably, this research encompasses several types of biomass residues, typically found in south-Europe regions, that typically do not receive enough attention in the literature but are produced in high quantities and must be sustainably managed. This uncommon focus on conducting a combined analysis of operational conditions, especially diverse under-represented biomass sources lends uniqueness to this study. For instance, in the review studies conducted by Dhyani and Bhaskar,<sup>35</sup> Afraz *et al.*,<sup>36</sup> and Marianela,<sup>37</sup> a wide range of different residual biomasses are compiled for pyrolysis analysis, but do not include several biomasses studied in this research.

Therefore, this new information provides a set of systematic information and knowledge on residual biomass pyrolysis under different operating conditions, which can support decisions related to pyrolysis projects, including the scale-up of the process for industrial production of different products with various potential applications. Furthermore, this study aims to promote efficient and targeted pyrolysis as a strategic approach for residual biomass management, particularly the residual biomass from forestry maintenance operations. This approach can contribute to better management of residual biomass from forestry operations for wildfire prevention in regions of southern Europe such as Portugal, and can also contribute to promoting the development of a local forestry-based economy in rural areas.

## 2. Materials and methods

### 2.1. Feedstock characterization

In this work, a set of distinct residual biomass types commonly found in the Portuguese forest and agroforest was used, and includes acacia (*Acacia longifolia*, A), gorse (*Ulex minor*, G), giant reed (*Arundo donax*, GR), olive pomace (OP), eucalyptus sawdust (ES) and eucalyptus bark (EB) (Fig. 1).





Fig. 1 Biomass samples. (a) acacia; (b) gorse; (c) giant reed; (d) olive pomace; (e) eucalyptus sawdust; (f) eucalyptus bark.

These feedstocks were selected for the following reasons: acacia, gorse and giant reed are available in Mediterranean forests and are available as a result of forestry maintenance operations for wildfire prevention, and acacia, being an invasive species, is subject to periodic removal as part of forestry operations; olive pomace is an agro-industrial by-product that is produced in large quantities in Portugal from olive oil extraction; eucalyptus sawdust and eucalyptus bark are two by-products of the pulp industry.

The raw feedstocks were pre-dried under atmospheric conditions (air dried) and sieved to a particle size between 2 and 4 mm.

The feedstocks were characterized for proximate analysis (Table 1) according to CEN/TS standards (14774-3:2004 for

moisture, 14775:2004 for ash, and 15148:2005 for volatile matter), ultimate analysis (C, H, N, and S) according to ISO 16948 and lower heating value (LHV) according to ISO 18125. The fixed carbon was determined by subtracting the sum of the percentages of ash and volatile matter from 100%, and the O content was calculated by subtracting the sum of the percentages of C, H, N, S and ashes from 100%.

## 2.2. Experimental setup

The experimental setup (Fig. 2) developed at the University of Aveiro (Portugal) used in this work includes a fixed-bed tubular quartz reactor with 20 mm internal diameter and 350 mm length; a tubular furnace that is controlled by an electronic unit that allows the regulation of heating rates and temperatures of the tubular quartz reactor; a thermocouple type K located at the central region of the quartz tube reactor in order to monitor the temperature of the biomass and feedback of the electronic control unit that controls the temperature of the electric furnace.

In each pyrolysis experiment (batch operation), a pre-weighed feedstock sample is placed inside a quartz tube, which is then inserted inside the electric furnace. Nitrogen gas (flow rate of  $0.150 \text{ L}_{\text{NPT}} \text{ min}^{-1}$ ) is used as the reactor purge gas in order to avoid the presence of oxygen and to carry the pyrolysis vapors that are released during the process. To perform the experiment, the electronic control system is switched on for operation of the electric furnace and heating the quartz reactor at the desired pre-programmed heating rate from ambient temperature until the pre-defined process temperature was reached, referred to in this work as the pyrolysis temperature, and maintained for the established soak time (30 minutes).

The pyrolysis vapors are transported to a set of condensers (Fig. 2j), where the fraction of these vapors is condensed (at  $\approx 273 \text{ K}$  and  $1.013 \times 10^5 \text{ Pa}$ ) to generate bio-oil, and the remaining gas (here referred to as permanent gas) flows to an exhaust system or is collected in a sampling bag. After the

Table 1 Proximate and ultimate analysis of biomass types used in the pyrolysis experiments in a laboratory scale fixed bed reactor

| Feedstocks   | A <sup>a</sup> | G <sup>a</sup> | GR <sup>a</sup> | OP <sup>a</sup> | ES <sup>a</sup> | EB <sup>a</sup> |
|--|----------------|----------------|-----------------|-----------------|-----------------|-----------------|
| <b>Proximate analysis</b>                            |                |                |                 |                 |                 |                 |
| Moisture (%wt., wb <sup>a</sup> )                    | 10.9           | 10.9           | 10.3            | 9.1             | 12.2            | 10.2            |
| Volatile matter (%wt., db <sup>a</sup> )             | 85.4           | 81.7           | 87.0            | 74.8            | 87.3            | 80.8            |
| Fixed carbon (%wt., db <sup>a</sup> )                | 12.5           | 16.9           | 9.4             | 19.8            | 11.9            | 14.6            |
| Ash (%wt., db <sup>a</sup> )                         | 2.1            | 1.4            | 3.6             | 5.4             | 0.8             | 4.6             |
| <b>Ultimate analysis (%wt., daf<sup>a</sup>)</b>     |                |                |                 |                 |                 |                 |
| C  | 52.5           | 50.4           | 51.0            | 53.5            | 51.4            | 50.0            |
| H  | 6.9            | 5.5            | 6.9             | 7.2             | 6.6             | 6.1             |
| N  | 1.1            | 0.7            | 0.6             | 1.3             | <0.1            | 0.3             |
| S  | Nd             | nd             | nd              | nd              | nd              | nd              |
| O  | 39.5           | 43.4           | 41.5            | 38.0            | 42.0            | 43.6            |
| LHV (MJ kg <sup>-1</sup> , db <sup>a</sup> )         | 20.1           | 18.2           | 19.4            | 20.3            | 19.8            | 18.0            |
| Bulk density (kg m <sup>-3</sup> , wb <sup>a</sup> ) | 154            | 197            | 141             | 672             | 138             | 80              |
| H/C molar ratio                                      | 1.6            | 1.3            | 1.6             | 1.6             | 1.6             | 1.5             |
| O/C molar ratio                                      | 0.6            | 0.6            | 0.6             | 0.5             | 0.6             | 0.7             |

<sup>a</sup> A – Acacia; G – gorse; GR – giant reed; OP – olive pomace; ES – eucalyptus sawdust; EB – eucalyptus bark. wb – wet basis; db – dry basis; daf – dry ash free.



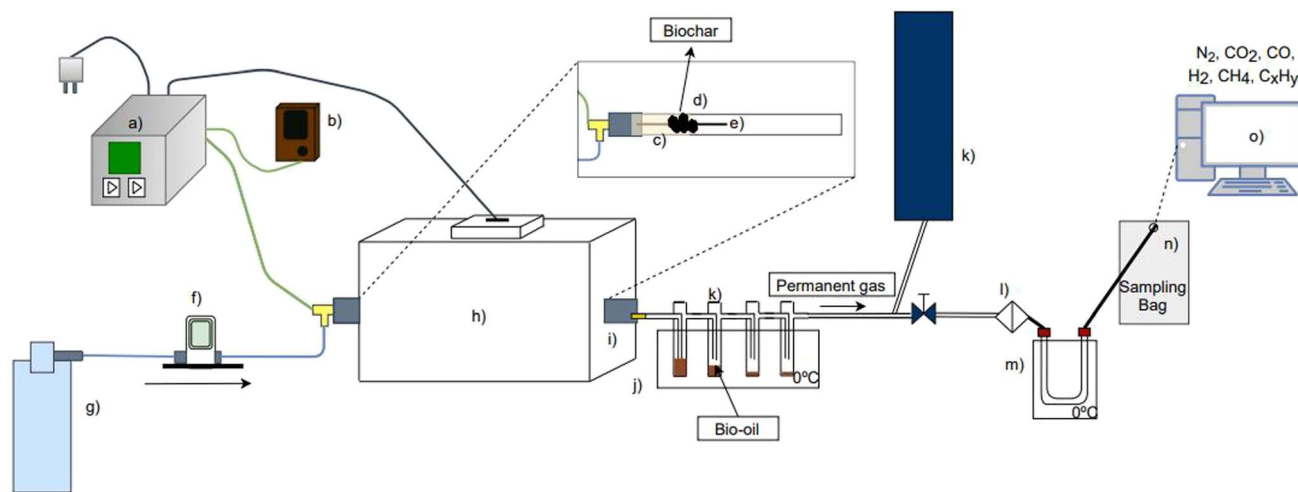


Fig. 2 Schematic representation of the experimental setup used. (a) Furnace controller; (b) datalogger recorder for temperature; (c) ceramic wool; (d) quartz tube; (e) thermocouple type K; (f) gas-flow controller; (g) N<sub>2</sub> cylinder; (h) electrical furnace; (i) vapor outlet; (j) pyrolysis vapor condensation unit with impingers for condensable gases (bio-oil); (k) exhaust system; (l) paper filter; (m) additional gas condensation unit for moisture and other condensable gases; (n) sampling bag; (o) gas chromatograph.

soaking time, the quartz tube reactor is removed from the furnace and left under room temperature conditions for cooling, under nitrogen purge.

### 2.3. Methodology

The pyrolysis experiments were performed to determine the effect of temperature, heating rate and biomass type on the yield of pyrolytic products (biochar, bio-oil, and permanent gas), and on biochar and permanent gas composition. The operating conditions of the pyrolysis experiments performed are detailed in Table 2.

The variation in biomass loading is a result of the strategy to achieve a consistent temperature profile in all experiments within the quartz tubular reactor. As the reactor exhibits a temperature gradient along its length, with lower temperatures at the begin and end sides of the reactor due to heat loss, the central zone of the reactor was selected based on the temperature profile uniformity to ensure it matched the desired experimental conditions. Consequently, the biomass loading in the quartz tubular reactor varies directly with volumetric mass. For example, olive pomace (OP) has a significantly higher volumetric mass compared to other types of biomasses, resulting in a higher amount of sample used in the reactor, in each experimental run.

The choice of temperatures, 350, 450 and 550 °C was based on literature information on the thermal decomposition ranges of the biomass macro-components (hemicellulose, cellulose and lignin),<sup>3,7,38,39</sup> and also based on previous studies of the pyrolysis process of other biomass materials.<sup>27</sup> According to the literature,<sup>3,7,38,39</sup> xylan, which is a frequently used model compound for studying hemicellulose pyrolysis, begins to degrade in the range of 220 to 350 °C. Cellulose, being more stable compared to hemicellulose, starts to decompose between 275 and 400 °C, with a peak in the mass loss rate at around 370 °C.

On the other hand, lignin is the most stable component and has a broad temperature decomposition range, varying between 200 and 500 °C. For this reason, a minimum pyrolysis temperature of 350 °C and a maximum temperature of 550 °C were defined to cover these degradation ranges to analyze the effect of temperature on pyrolysis product yields and biochar and permanent gas composition.

Regarding heating rates, these were selected based on literature studies of slow and intermediate pyrolysis for biochar and bio-oil production<sup>34,40</sup> and on previous experience of biomass pyrolysis studies in the reactor used.<sup>27</sup>

For each experiment, the amount of biomass batch loaded and the amount of biochar and bio-oil produced were quantified. The mass of permanent gas was determined using a mass balance in the pyrolysis process, following eqn (1):

$$m_{\text{gas}} = m_{\text{bm,wb}} - m_{\text{biochar}} - m_{\text{bio-oil}} \quad (1)$$

The yield of products on a biomass dry basis was determined following eqn (2)–(4):

$$Y_{\text{biochar,db}} = \frac{m_{\text{biochar,db}}}{m_{\text{bm,db}}} \quad (2)$$

$$Y_{\text{bio-oil,db}} = \frac{m_{\text{bio-oil}} - (m_{\text{bm,wb}} - m_{\text{bm,db}})}{m_{\text{bm,db}}} \quad (3)$$

$$Y_{\text{gas,db}} = \frac{m_{\text{gas,db}}}{m_{\text{bm,db}}} \quad (4)$$

It should be noted that in the calculation of the bio-oil yield determined through eqn (3), the contribution of the condensed water originating from biomass moisture was discounted, and only the condensed water originating from the pyrolytic reactions (pyrolytic water) is taken into account for the amount of bio-oil yield.





**Table 2** Pyrolysis experiment reference and respective operating conditions. Experiments under N<sub>2</sub> gas flow (0.15 L<sub>NPT</sub> min<sup>−1</sup>) and 30 minutes of soaking time

| Reference | Feedstock          | Pyrolysis temperature (°C) | Heating rate (°C min <sup>−1</sup> ) | Biomass load (g, wb) |
|-----------|--------------------|----------------------------|--------------------------------------|----------------------|
| A,350,2   | Acacia             | 350                        | 2                                    | ≈ 4.5                |
| A,450,2   | Acacia             | 450                        |                                      |                      |
| A,550,2   | Acacia             | 550                        |                                      |                      |
| A,350,10  | Acacia             | 350                        | 10                                   |                      |
| A,450,10  | Acacia             | 450                        |                                      |                      |
| A,550,10  | Acacia             | 550                        |                                      |                      |
| G,350,2   | Gorse              | 350                        | 2                                    | ≈ 5.0                |
| G,450,2   | Gorse              | 450                        |                                      |                      |
| G,550,2   | Gorse              | 550                        |                                      |                      |
| G,350,10  | Gorse              | 350                        | 10                                   |                      |
| G,450,10  | Gorse              | 450                        |                                      |                      |
| G,550,10  | Gorse              | 550                        |                                      |                      |
| GR,350,2  | Giant reed         | 350                        | 2                                    | ≈ 3.5                |
| GR,450,2  | Giant reed         | 450                        |                                      |                      |
| GR,550,2  | Giant reed         | 550                        |                                      |                      |
| GR,350,10 | Giant reed         | 350                        | 10                                   |                      |
| GR,450,10 | Giant reed         | 450                        |                                      |                      |
| GR,550,10 | Giant reed         | 550                        |                                      |                      |
| OP,350,2  | Olive pomace       | 350                        | 2                                    | ≈ 15.5               |
| OP,450,2  | Olive pomace       | 450                        |                                      |                      |
| OP,550,2  | Olive pomace       | 550                        |                                      |                      |
| OP,350,10 | Olive pomace       | 350                        | 10                                   |                      |
| OP,450,10 | Olive pomace       | 450                        |                                      |                      |
| OP,550,10 | Olive pomace       | 550                        |                                      |                      |
| ES,350,2  | Eucalyptus sawdust | 350                        | 2                                    | ≈ 5.0                |
| ES,450,2  | Eucalyptus sawdust | 450                        |                                      |                      |
| ES,550,2  | Eucalyptus sawdust | 550                        |                                      |                      |
| ES,350,10 | Eucalyptus sawdust | 350                        | 10                                   | ≈ 5.0                |
| ES,450,10 | Eucalyptus sawdust | 450                        |                                      |                      |
| ES,550,10 | Eucalyptus sawdust | 550                        |                                      |                      |
| ES,350,30 | Eucalyptus sawdust | 350                        | 30                                   |                      |
| ES,450,30 | Eucalyptus sawdust | 450                        |                                      |                      |
| ES,550,30 | Eucalyptus sawdust | 550                        |                                      |                      |
| EB,350,2  | Eucalyptus bark    | 350                        | 2                                    | ≈ 3.5                |
| EB,450,2  | Eucalyptus bark    | 450                        |                                      |                      |
| EB,550,2  | Eucalyptus bark    | 550                        |                                      |                      |
| EB,350,10 | Eucalyptus bark    | 350                        | 10                                   |                      |
| EB,450,10 | Eucalyptus bark    | 450                        |                                      |                      |
| EB,550,10 | Eucalyptus bark    | 550                        |                                      |                      |
| EB,350,30 | Eucalyptus bark    | 350                        | 30                                   |                      |
| EB,450,30 | Eucalyptus bark    | 450                        |                                      |                      |
| EB,550,30 | Eucalyptus bark    | 550                        |                                      |                      |

The biochars were characterized for proximate analysis following CEN/TS standards (14774-3:2004 for moisture, 14775:2004 for ash, and 15148:2005 for volatile matter), ultimate analysis (C, H, N, and S) following ASTM D5373 and the lower heating value following ASTM D5865. The O content was calculated by using difference of the sum of the mass percentages of C, H, N, S and ashes and 100%.

The dry permanent gas composition (H<sub>2</sub>, CH<sub>4</sub>, CO, CO<sub>2</sub>, C<sub>2</sub>H<sub>4</sub>, C<sub>2</sub>H<sub>6</sub>, and C<sub>3</sub>H<sub>8</sub> molar concentration) was characterized following gas sampling in bags (FlexFoil) and its analysis using a gas chromatograph. The LHV of the dry permanent gas was determined based on its composition, namely the concentration of combustible gases (H<sub>2</sub>, CH<sub>4</sub>, CO, C<sub>2</sub>H<sub>4</sub>, C<sub>2</sub>H<sub>6</sub>, and C<sub>3</sub>H<sub>8</sub>) and their respective LHV (under reference conditions, 298 K

and 1.013 × 10<sup>5</sup> Pa). The bio-oil samples collected will be further characterized in future studies.

### 3. Results and discussion

The results presented in this section include the biochar, bio-oil and permanent gas yields, and biochar and permanent gas composition (proximate and ultimate analysis, and the LHV of biochar, and the concentration of CO, CO<sub>2</sub>, CH<sub>4</sub>, C<sub>2</sub>H<sub>4</sub>, C<sub>2</sub>H<sub>6</sub>, C<sub>3</sub>H<sub>8</sub>, and H<sub>2</sub> and the LHV of permanent gas), produced in the bench-scale fixed bed pyrolysis reactor. The focus is the study and analysis of the influence of operating conditions, namely, pyrolysis temperature, heating rate, and feedstock type on the pyrolysis product distribution and composition.



### 3.1. Yield and composition of biochar

Fig. 3 shows samples of biochar produced in pyrolysis experiments conducted at 450 °C and a heating rate of 10 °C min<sup>-1</sup> for different biomass types.

The impact of the temperature and heating rate on biochar yield is shown in Fig. 4. In some situations, the error bars are virtually absent due to minimal variation between replicates (less than 1%).

The biochar yield was between 0.22 and 0.47 kg kg<sup>-1</sup> dry biomass, which are within the range of typical values for the slow pyrolysis process under similar conditions.<sup>12–14</sup> Increasing the pyrolysis temperature resulted in a decrease in biochar yield (resulting in an average reduction of 24% in biochar yield), attributed to the higher temperatures favoring the thermochemical decomposition of biomass, consequently increasing the release of volatile matter.<sup>2,17</sup> Increasing the heating rate also reduced biochar yield (5% on average), though the effect was less pronounced than that of temperature.

The type of biomass had an impact on biochar yield, with pyrolysis of olive pomace producing higher biochar yields, while eucalyptus sawdust resulted in lower biochar yields, resulting in an average difference of 22%. This can be justified by the higher content of ash, fixed carbon and density of the olive pomace, while eucalyptus sawdust presents a higher volatile matter content, finer particles (Fig. 1) and low density, which may have contributed to a higher release of compounds into the gas phase, leading to a lower mass of biochar.<sup>7</sup> The effect of chemical composition (*e.g.*, volatile matter content) on biochar yield and composition is discussed in section 3.4.

The average contents of ash, fixed carbon (FC), and volatile matter (VM) of the biochar produced are shown in Fig. 5. In general, it is observed that the relationship between these components and the increase in heating rate do not follow a clear trend, unlike what occurs with the increase in temperature, as detailed below. This is in line with results typically observed in the literature.<sup>27</sup>

The increase in ash content of biochar with the temperature is a consequence of the higher thermochemical decomposition of the organic fraction of biomass, which is converted into pyrolysis vapors, thus resulting in the enrichment of inorganic elements (ash) in the biochar. This is a result of these organic elements having low volatility at the temperatures used in the pyrolysis process. This biochar enrichment in ash (inorganic elements) is of the order of 1.2 to 5.1 times the value of ash present in the parent biomass (db). The decrease in volatile matter content of the biochar with the increase in pyrolysis temperature is also explained as a result of the increase in the thermochemical decomposition of the organic fraction of biomass at higher temperatures and its consequent release to the gas phase.<sup>41</sup> There is also a trend for an increase in the FC content of biochar with an increase in temperature, and that is a result of a balance between volatile matter and ash contents of the biochar.

The higher values of ash content in biochar were found for pyrolysis of olive pomace (13.2 %wt. db) at a temperature of 550 °C and heating rate of 2 °C min<sup>-1</sup> and for pyrolysis of eucalyptus bark (10.0 %wt. db) at 550 °C and 30 °C min<sup>-1</sup>. These higher values of ash in biochar from olive pomace and eucalyptus bark are explained by the higher ash content present in the raw biomass (Table 1). The lowest ash content (1.1 %wt. db) is observed in the biochar produced from eucalyptus sawdust at 350 °C and 10 °C min<sup>-1</sup>, and this can also be explained by the lower ash content of raw biomass (Table 1).

Regarding VM content of biochar, the highest content (58.1 %wt., biochar db) is observed for biochar from pyrolysis of eucalyptus sawdust at 350 °C and 2 °C min<sup>-1</sup>, and this can be explained as being related to the higher VM content present in raw biomass (Table 1). The lowest VM content (12.4 %wt., dry biochar) is found in the biochar produced from pyrolysis of olive pomace at 550 °C and 2 °C min<sup>-1</sup>, and this can be explained as related to the lower VM content and higher ash content present in raw biomass (Table 1).

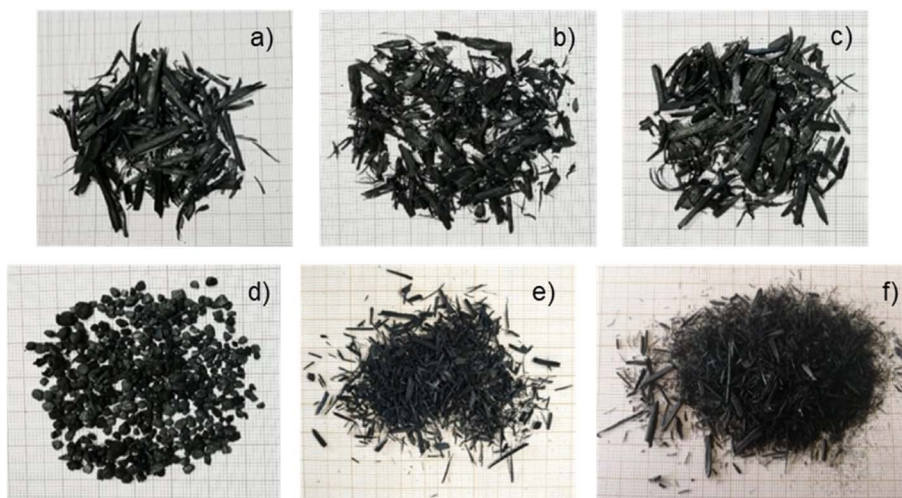


Fig. 3 Biochar samples produced at 450 °C and 10 °C min<sup>-1</sup> from experiments; (a) A,450,10; (b) G,450,10; (c) GR,450,10; (d) OP,450,10; (e) ES,450,10; (f) EB,450,10. Experiment reference following Table 2.



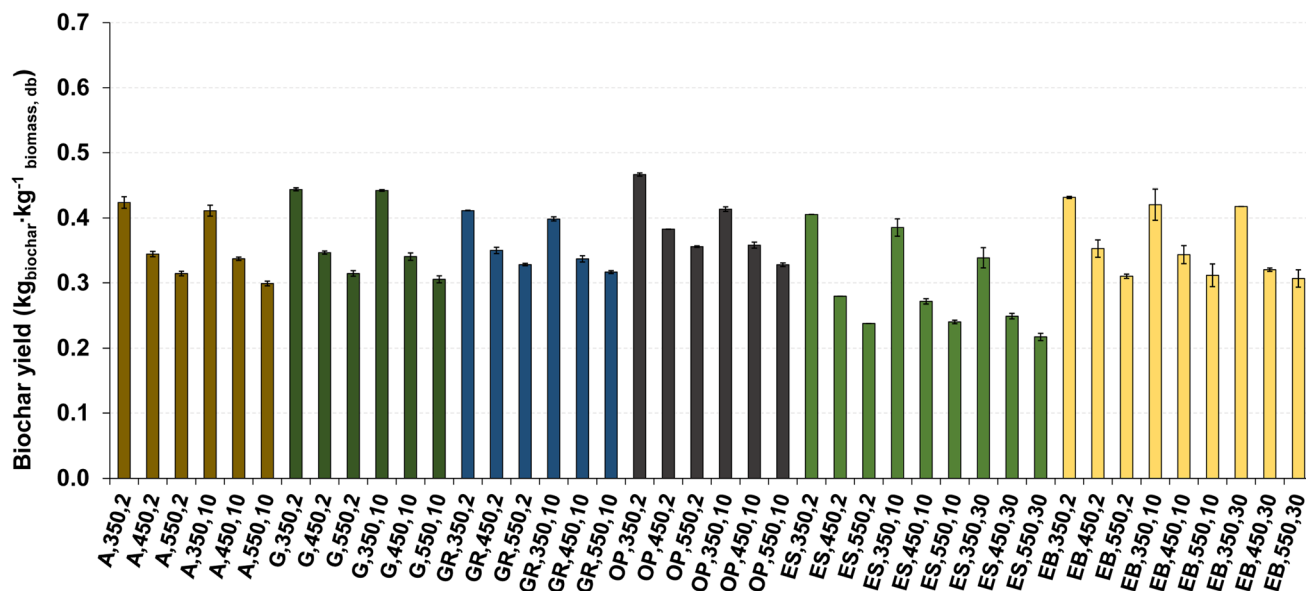


Fig. 4 Biochar yield for pyrolysis of different biomass types under distinct operating conditions. Reference of experiments in the X-axis following nomenclature in Table 2.

Ultimate analysis (C, H, N, and O concentration) and the LHV of some biochar samples produced are presented in Fig. 6 and 7, respectively. The selection of these specific biochar samples aimed to provide an overview of responses under different pyrolysis conditions, covering thermochemical decomposition conditions from low, to intermediate, and extreme within the range used in this work.

The C content of biochar samples is higher than  $0.69 \text{ kg kg}^{-1}$  dry biochar, thus fulfilling the European Biochar Certificate (EBC)<sup>42</sup> criteria on C concentration (higher than  $0.50 \text{ kg organic carbon kg}^{-1}$  dry biochar) to be classified as biochar for soil application. However, this guideline only considers the organic

carbon content and does not include the inorganic carbon in biochar. In biochar, inorganic carbon is mostly in the form of carbonates such as calcite.<sup>43</sup> Therefore, the presence of calcium in the biochar ash could be an indication of the presence of inorganic carbon in biochar. According to the literature for residual eucalyptus biomass, which has physico-chemical properties similar to those of the biomass studied in this work, the Ca concentration in the ash is very low, ranging between 7910 and 9480 ppm wt., db.<sup>44</sup> Therefore, even with its enrichment in the biochar through the pyrolysis process, the Ca concentration will continue to be very low and of low relevance compared to the total carbon concentration in the biochar

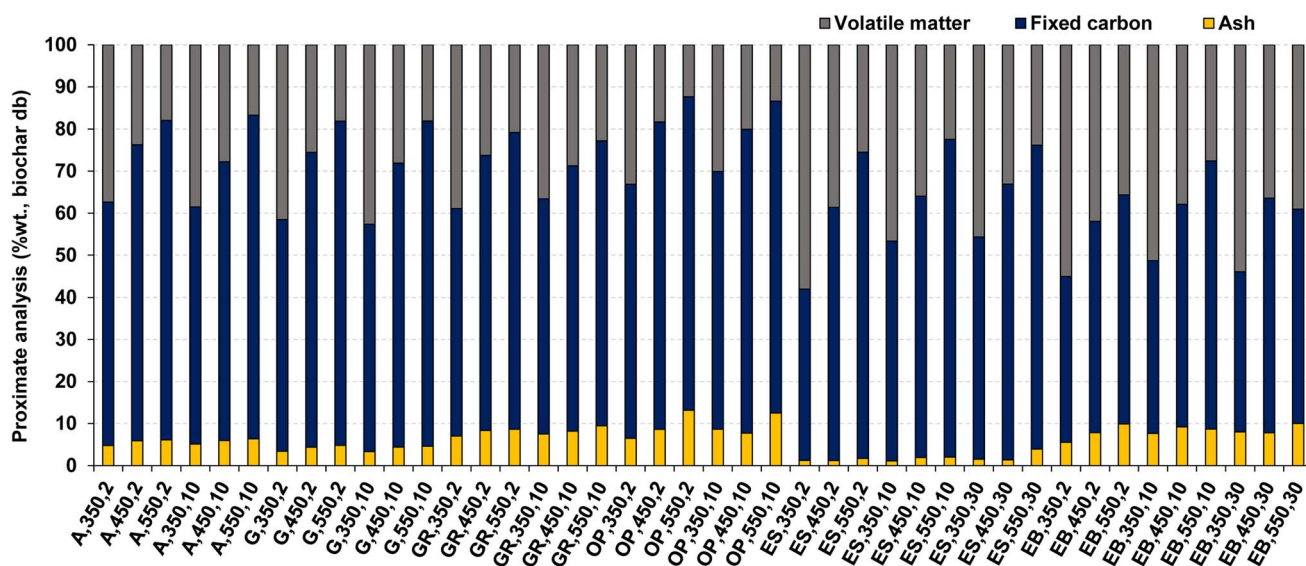


Fig. 5 Proximate analysis of the biochar produced in the pyrolysis experiments. Reference of experiments in the X-axis following nomenclature in Table 2.



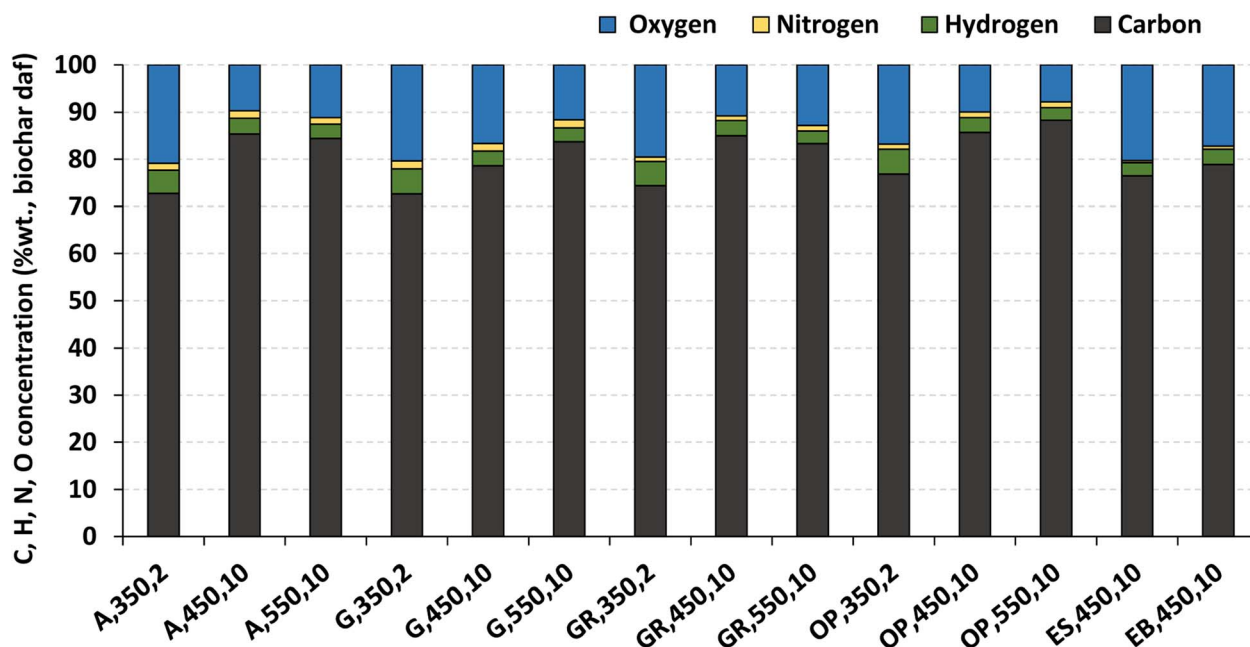


Fig. 6 Ultimate analysis (C, H, N, and O concentration on a dry and ash free (daf) basis) of the biochar produced by pyrolysis of different biomass types under distinct operating conditions. Reference of experiments in the X-axis following nomenclature in Table 2.

(more than  $0.69 \text{ kg kg}^{-1} \text{ db}$ ). Therefore, in this study, the total carbon concentration was compared with the organic carbon EBC guideline.

The biochar produced from pyrolysis of olive pomace at  $550^\circ \text{C}$  and  $10^\circ \text{C min}^{-1}$  has a higher carbon content ( $88.3\% \text{ wt.}$ , dry ash free basis of biochar). The biochar produced from pyrolysis of gorse at  $350^\circ \text{C}$  and  $2^\circ \text{C min}^{-1}$  has the minimum carbon content ( $72.6\% \text{ wt.}$ , dry ash free of biochar). Under the same operating conditions of temperature ( $450^\circ \text{C}$ ) and heating rate ( $10^\circ \text{C min}^{-1}$ ), the maximum carbon content of biochar is

obtained for biochar produced from olive pomace and acacia ( $85.7\% \text{ wt.}$  and  $85.4\% \text{ wt.}$ , dry ash free basis of biochar, respectively), and this can be explained by the higher carbon content of the respective raw biomass samples (Table 1). In relation to the effect of temperature, and for the same heating rate, no clear pattern is observed for the elemental (C, H, N, and O) composition of biochar (Fig. 6).

The LHV of biochar was in the range from  $24.2$  to  $30.5 \text{ MJ kg}^{-1}$  (dry biochar basis). These values surpass the range of the LHV of raw biomass ( $16.7$  to  $19.3 \text{ MJ kg}^{-1}$  of dry biomass, Table

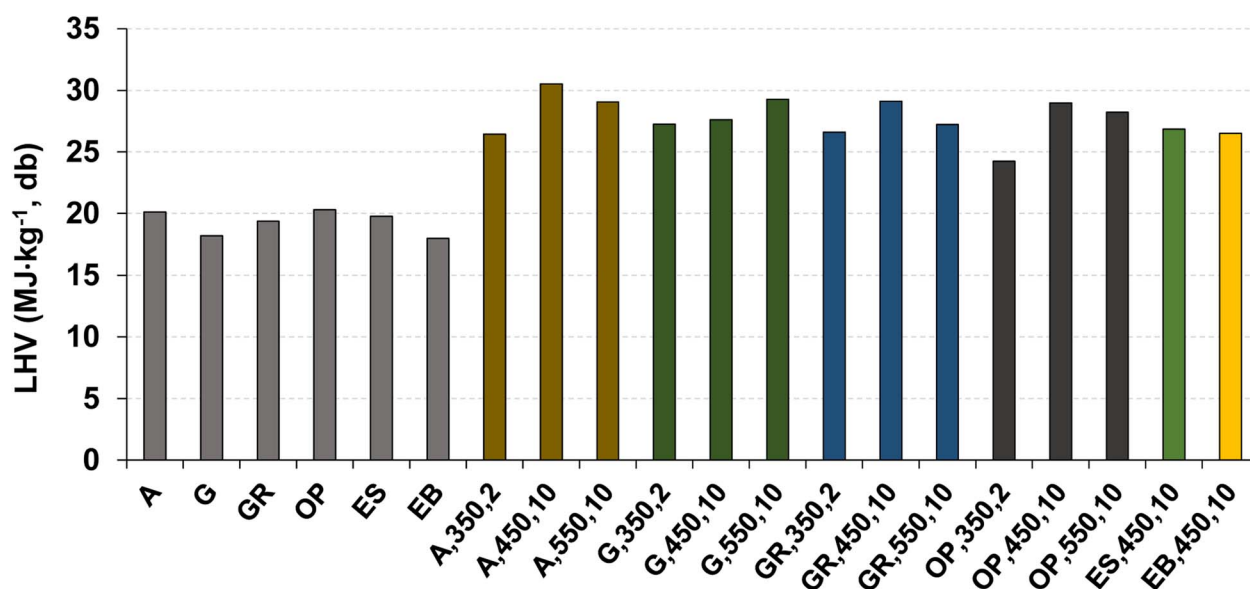


Fig. 7 Lower heating value of the biomass and respective biochar samples produced by pyrolysis under distinct operating conditions. Reference of experiments in the X-axis following nomenclature in Table 2.





1), primarily due to reduced oxygen content and the respective increase in C content.<sup>45</sup> For the same operating conditions of temperature (450 °C) and heating rate (10 °C min<sup>-1</sup>), a higher LHV is observed for biochar of acacia, which has a higher C and a lower O concentration compared to the biochar obtained from the other biomass types used.

These distinctive properties of biochar, including its ash content, carbon composition, and high calorific value, have significant implications for its potential applications. The increase in inorganic content in biochar can be particularly relevant when considering its use as a soil amendment, enriching the soil with essential nutrients for plant growth. Therefore, biochar produced through pyrolysis at higher temperatures and heating rates may be a valuable option for enhancing agricultural practices and, consequently, soil quality. However, it is important to note that adhering to the guidelines of the European Biochar Certificate (EBC) requires a comprehensive analysis, going beyond organic carbon content, to thoroughly analyze, for example, the inorganic constituents of biochar. This underscores the need for further investigation in this area.

Furthermore, when biochar is incorporated into the soil, the carbon present in its solid matrix is stored as stable organic matter, remaining retained for extended periods. This characteristic makes biochar an effective tool for carbon sequestration, playing a fundamental role in reducing carbon dioxide (CO<sub>2</sub>) concentrations in the atmosphere.

On the other hand, biochar also presents additional attributes relevant to energy related applications. It has high calorific values, comparable to or even higher than that of fossil-origin coal (20.3–30.1 MJ kg<sup>-1</sup> (ref. 46)), high carbon content, and low levels of nitrogen and sulfur. This offers promising prospects in the energy sector, including heat and electricity generation. However, it's important to acknowledge that the elevated ash content in biochar may pose challenges in such applications, potentially resulting in issues like slag formation and corrosion.<sup>47</sup>

Additionally, the high carbon content of char also highlights the potential for it to be processed and converted into activated carbons for use in other types of applications, such as energy storage materials like electrodes, catalysts for thermochemical processes, and adsorbents.<sup>47,48</sup> However, other characteristics must be analyzed according to the specific application, such as specific surface area,<sup>47</sup> and therefore, further analyses are required in this context.

### 3.2. Yield of bio-oil

Fig. 8 shows bio-oil samples collected in impingers (condensers) during pyrolysis experiments at 450 °C and a heating rate of 10 °C min<sup>-1</sup>.

The influence of pyrolysis temperature and heating rate on the bio-oil yield is illustrated in Fig. 9.

The bio-oil yield is in the range of 0.26 and 0.59 kg kg<sup>-1</sup> dry biomass, slightly higher than the typical values reported in the literature for the slow pyrolysis process.<sup>19,27,49–51</sup> The highest bio-oil yield (0.59 kg kg<sup>-1</sup> dry biomass) is obtained from pyrolysis of eucalyptus sawdust at 450 °C and 30 °C min<sup>-1</sup>, as well as at



Fig. 8 Bio-oil collected in the first condenser of the experimental setup (Fig. 2) for pyrolysis of acacia (a), olive pomace (b) and eucalyptus bark (c).

550 °C and 30 °C min<sup>-1</sup>, and this can be explained as a result of the higher content of volatile matter (see section 3.4), low ash content and low bulk density of eucalyptus sawdust. The lowest bio-oil yield (0.26 kg kg<sup>-1</sup> dry biomass) is observed for the pyrolysis of giant reed at 550 °C and 2 °C min<sup>-1</sup>.

For the same heating rate, increasing the temperature resulted in an increase (15% on average) in bio-oil yield, while at the same temperature, increasing the heating rate resulted in an increase (21% on average) of bio-oil yield. As already mentioned in subsection 3.1, this can be explained by the increased extent of primary thermochemical decomposition reactions that promote the formation of more pyrolysis vapors. However, the experiments conducted at a heating rate of 2 °C min<sup>-1</sup> showed an increase in bio-oil yield as the temperature increased from 350 to 450 °C, followed by a decrease as the temperature increased from 450 to 550 °C. This behavior can be explained as a result of the longer experiment time (about 5 hours), which promoted secondary reactions between the solids and vapors, leading to a decrease in the yield of condensable vapors and precursors of bio-oil, and an increase in the yield of non-condensable vapors (permanent gas).<sup>52</sup>

### 3.3. Yield and composition of permanent gas

The influence of pyrolysis temperature and heating rate on the permanent gas yield is shown in Fig. 10. The permanent gas yield is dependent on biochar and bio-oil yield, because it is determined by difference between the mass of biomass and the sum of the corresponding measured mass of biochar and bio-oil produced, following eqn (1) and (4) in section 2.3.

The permanent gas yield is between 0.17 and 0.41 kg kg<sup>-1</sup> dry biomass. The highest permanent gas yield (0.41 kg kg<sup>-1</sup> dry biomass) is obtained from the pyrolysis of giant reed at 550 °C and 2 °C min<sup>-1</sup>, and the lowest value (0.17 kg kg<sup>-1</sup> dry



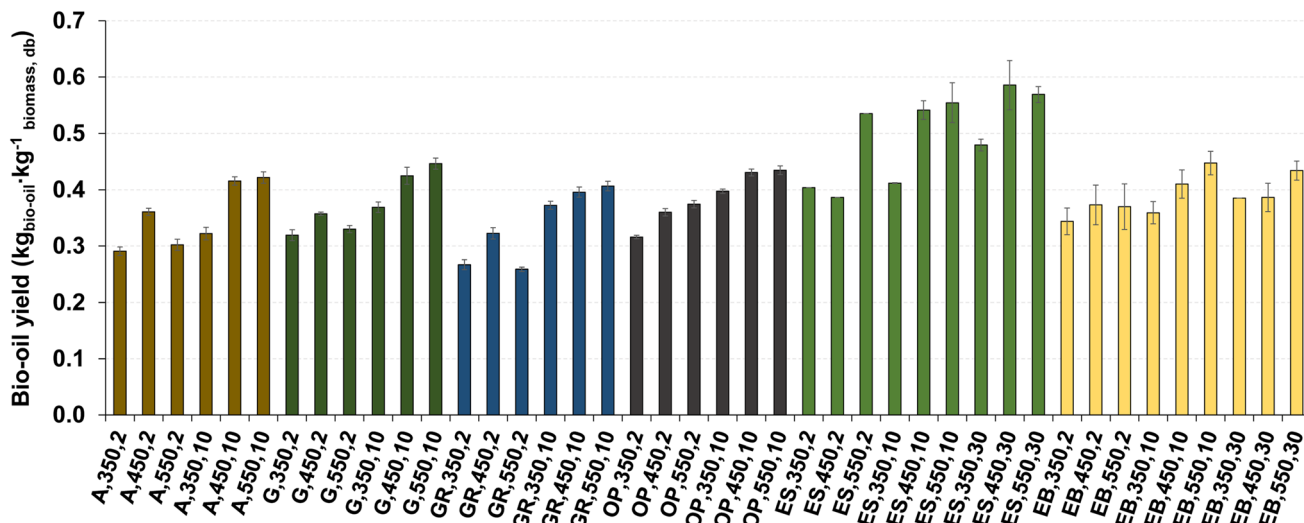


Fig. 9 Bio-oil yield for pyrolysis of different biomass types under distinct operating conditions. Reference of experiments in the X-axis following nomenclature in Table 2.

biomass) was achieved in the pyrolysis of eucalyptus sawdust at 450 °C and 30 °C min<sup>-1</sup>. For most of the experiments conducted with acacia, gorse, giant reed, and olive pomace, the permanent gas yield tends to increase with increasing temperature. In most of the pyrolysis experiments with different types of biomasses, the highest permanent gas yield is obtained at 550 °C and 2 °C min<sup>-1</sup>, except for eucalyptus sawdust. This phenomenon may be related to the increased extent of secondary reactions of the vapors with solids because of the higher reaction time under these lower heating rate conditions as explained in subsection 3.4 and also referred to in the literature.<sup>52</sup>

Nevertheless, the effect of temperature and heating rate on permanent gas yield showed no clear trends and

depended on the biomass type. Remarkably, in the case of residual biomass from eucalyptus, particularly in eucalyptus sawdust (ES), behaviors of pyrolysis product yield distinct from that of other biomass types were observed, and these may be related to the shape of biomass particles, which can influence the heating rate and the mechanisms of biomass decomposition.

The influence of pyrolysis temperature, heating rate and biomass type on the permanent gas composition (expressed as %v CO<sub>2</sub>, CO, CH<sub>4</sub>, H<sub>2</sub>, C<sub>2</sub>H<sub>6</sub>, C<sub>3</sub>H<sub>8</sub>, and C<sub>2</sub>H<sub>4</sub>, on a dry basis and inert gas free) and permanent gas LHV is shown in Fig. 11 and 12 for some experiments where the characterization of permanent gas composition was made. Specific

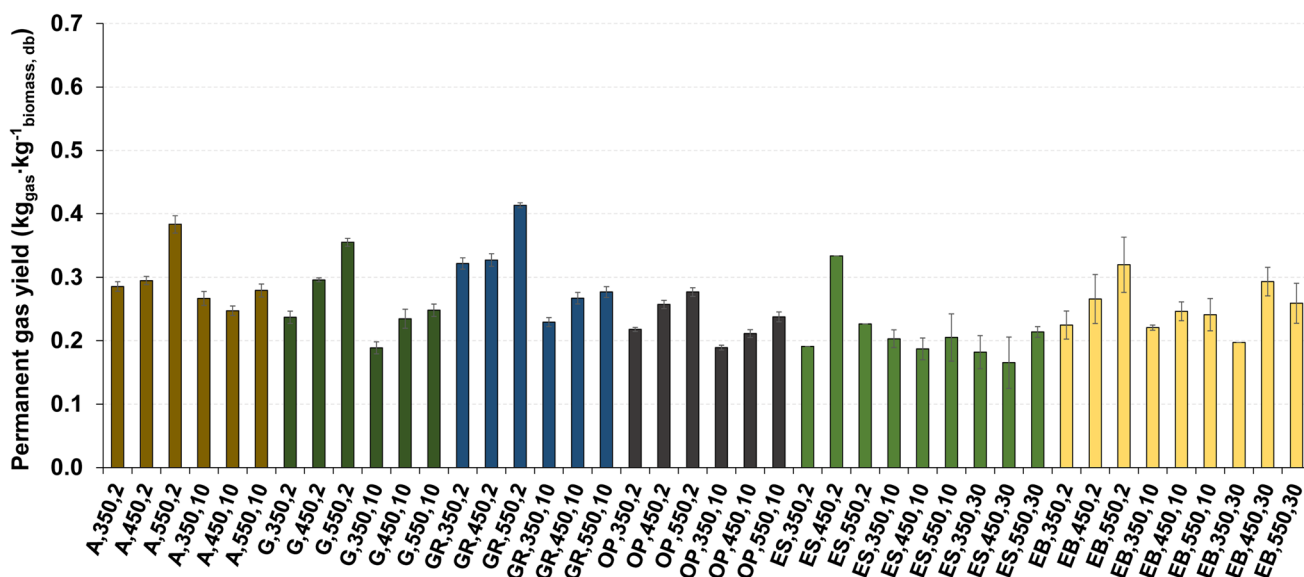


Fig. 10 Permanent gas yield for pyrolysis of different biomass types under distinct operating conditions. Reference of experiments in the X-axis following Table 2.



conditions were chosen to provide an overview of the effect of pyrolysis conditions within the range used in this work.

CO<sub>2</sub> and CO are by far the major components of permanent gas, accounting for approximately 85 %v, with the remaining gaseous species (CH<sub>4</sub>, H<sub>2</sub>, C<sub>2</sub>H<sub>6</sub>, C<sub>3</sub>H<sub>8</sub>, and C<sub>2</sub>H<sub>4</sub>) making up less than 15 %v of the composition. With the same heating rate and biomass type, an increase in temperature (*e.g.*, from 450 °C to 550 °C, reference: ES,450,10 and ES,550,10) caused in a decrease in CO<sub>2</sub> and an increase in CH<sub>4</sub> and H<sub>2</sub> concentration in the permanent gas, consistent with other studies.<sup>8,53,54</sup> Conversely, maintaining the temperature and biomass type while increasing the heating rate (*e.g.*, from 10 °C min<sup>-1</sup> to 30 °C min<sup>-1</sup>, reference: ES,450,10 and ES,450,30) led to an increase in CO<sub>2</sub> and a decrease in CH<sub>4</sub> concentration in the permanent gas. It's important to note that the impact of the heating rate is less pronounced when compared to the influence of temperature.

For the set of pyrolysis experiments where the permanent gas composition was determined (Fig. 11), the LHV of that gas was in the range of 5.4 MJ Nm<sup>-3</sup> to 9.7 MJ Nm<sup>-3</sup> (Fig. 12). An increase in temperature led to an increase in the LHV (*e.g.*, from 8.3 to 9.7 MJ Nm<sup>-3</sup>, for experiments ES,450,10 and ES,550,10, respectively), mainly due to an increase in the concentrations of CH<sub>4</sub> and H<sub>2</sub>, which represents a substantial part of the energy content of the pyrolysis gas. The effect of the heating rate on the permanent gas composition and LHV was only evaluated for experiments with eucalyptus sawdust, at 450 °C and 550 °C, but no clear trend was observed. Additionally, under the same operating conditions of temperature (450 °C) and heating rate (10 °C min<sup>-1</sup>), a higher LHV of permanent gas is found for the pyrolysis of giant reed due to its higher CO and lower CO<sub>2</sub> concentration, in comparison to the permanent gas produced by other biomass types.

Therefore, increasing the pyrolysis temperature leads to an improvement in the quality of the permanent gas, making it a more suitable energy source for applications like

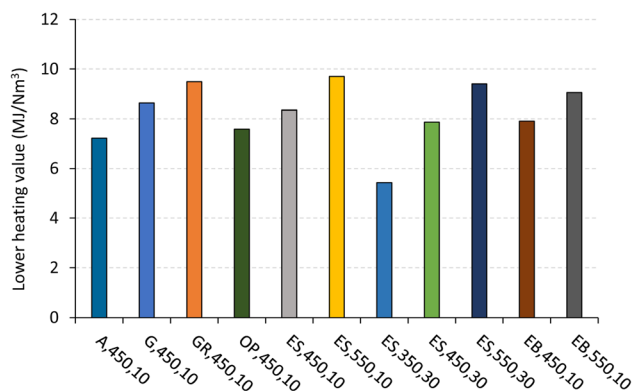


Fig. 12 Lower heating value of permanent gas produced by pyrolysis of biomass under different operating conditions. Reference of experiments in the X-axis following nomenclature in Table 2.

combustion to support the pyrolysis process or other related processes, such as biomass drying.<sup>45,55</sup> This relationship between temperature and a higher LHV has been observed in several biomass pyrolysis studies,<sup>8,13</sup> and can be explained by the increase in temperature promoting the secondary cracking of organic compounds into light gases, as previously discussed in section 3.1.

#### 3.4. Influence of biomass composition on pyrolysis product yield

The influence of biomass composition, particularly the FC and VM content, on the yields of biochar, vapors (bio-oil plus permanent gas) and bio-oil and permanent gas separately is shown in Fig. 13–16.

At a pyrolysis temperature of 350 °C, biomass with higher FC content tends to result in greater biochar yield (Fig. 13). This is because FC represents the fraction of the organic matrix in biomass that does not thermally decompose into gaseous products (volatiles) under inert heating conditions,

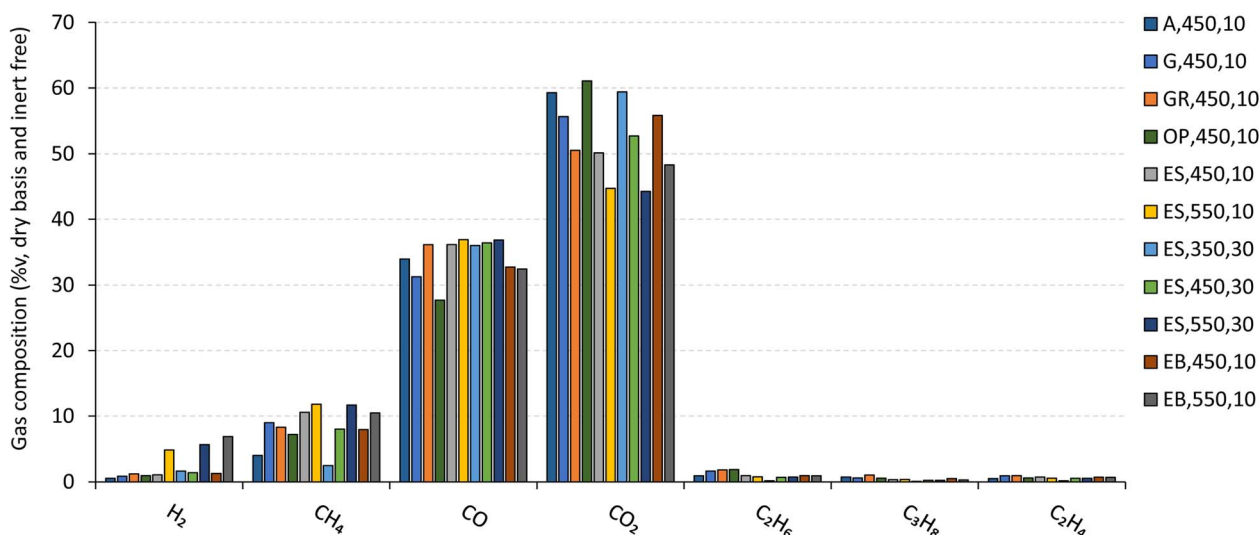


Fig. 11 Permanent gas composition (CO<sub>2</sub>, CO, CH<sub>4</sub>, H<sub>2</sub>, C<sub>2</sub>H<sub>4</sub>, C<sub>2</sub>H<sub>6</sub> and C<sub>3</sub>H<sub>8</sub>) produced by pyrolysis of biomass under different operating conditions. Reference of experiments in the legend follow nomenclature in Table 2.

making it the primary precursor to solid pyrolysis products such as char or biochar.<sup>7</sup> However, for other tested temperatures, although the general trend shows increased biochar yield with higher FC content, there's less clarity when comparing biomass types with similar FC contents (between 12 and 17 %wt., dry biomass). Other factors, including biomass particle size, shape, physical structure, and the influence of temperature on thermochemical decomposition, may overlap and influence the results.<sup>7</sup>

Regarding the pyrolysis vapor (bio-oil and permanent gas) yield shown in Fig. 14, it can be observed that higher VM content in biomass tends to promote higher vapor yield. However, some exceptions can be observed, as for example, the giant reed pyrolysis at 550 °C and 2 °C min<sup>-1</sup> and 10 °C min<sup>-1</sup>, and other reasons could be influencing the vapor release, *e.g.*, the overlap of other factors (temperature, size, shape, and physical structure of the biomass particles), and should be subjected to further studies.<sup>2,7</sup>

The increase in VM content in biomass appears to not have an unequivocal relation to the bio-oil yield, and a direct or an indirect relation can be found depending on the operating conditions (Fig. 15). Nevertheless, for VM content above 80 % wt. an indirect relation between VM and bio-oil yield seems to exist for several operating conditions.

On the other hand, it can be observed that the increase in VM content of biomass is related to an increase in permanent gas yield (Fig. 16). The pyrolysis of eucalyptus sawdust has a particular behavior that deviates from that of the other biomass types, namely, producing a higher bio-oil yield and a lower permanent gas yield when compared to biomass with a similar VM content. The reason for this behavior must be the subject of further studies, but perhaps is related to the smaller particle size of these biomass samples, which facilitates faster heating and promotes the release of pyrolysis vapors. These vapors are then able to escape from the particle before undergoing secondary reactions and forming light gases, resulting in a higher yield of bio-oil.

### 3.5. Effect of operating conditions on biochar composition

In this section, the effect of operating conditions on biochar composition was analyzed, specifically on the FC content, O/C and H/C molar ratios.

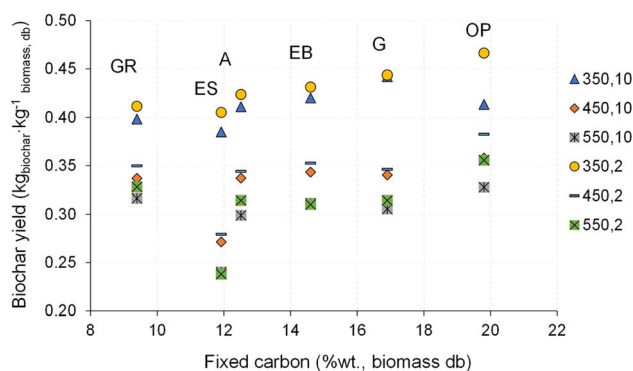


Fig. 13 Influence of FC content of biomass on the yield of biochar.

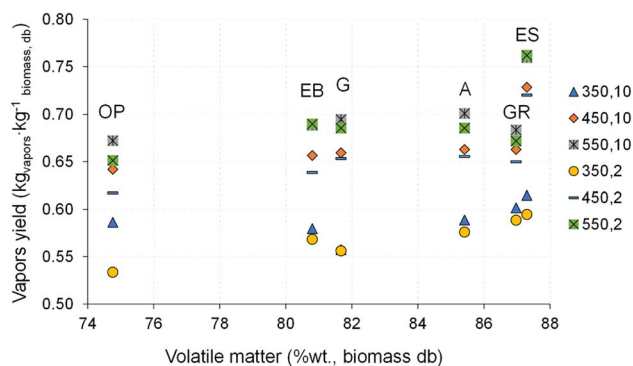


Fig. 14 Influence of VM content of biomass on the yield of pyrolysis vapors (bio-oil plus permanent gas).

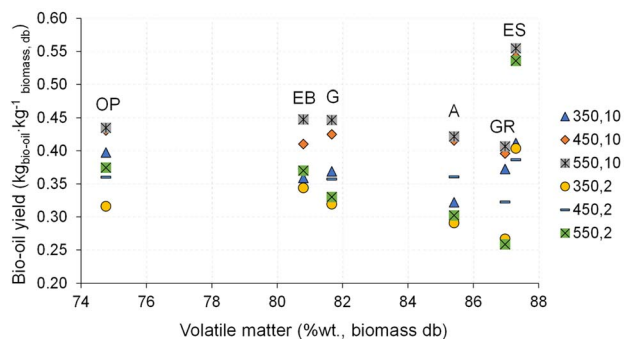


Fig. 15 Influence of VM content of biomass on the yield of bio-oil.

Fig. 17 demonstrates the influence of pyrolysis temperature, with a heating rate of 10 °C min<sup>-1</sup>, on the yield and FC content of biochar. It is clear that pyrolysis temperature strongly affects both biochar yield and FC content. As the temperature increases, biochar yield decreases, while the FC content of biochar increases. This behavior is consistent across different biomass types used (Fig. 17). The influence of temperature on these factors can be explained as a result of stronger thermochemical decomposition of biomass with increasing temperature, indicated by a higher release of VM (primary pyrolysis reaction) and the corresponding decrease in the mass yield of biochar, and an increase in the concentration of FC in biochar.<sup>7,8</sup>

The H/C and O/C molar ratios of raw biomass and the respective biochar produced in the pyrolysis experiments are represented in a Van Krevelen diagram in Fig. 18. These ratios offer insights into the degree of thermochemical conversion during dehydration and carbonization reactions. Lower H/C and O/C ratios mean a higher degree of carbonization and biochar stability.<sup>56,57</sup> In fact, H/C and O/C molar ratios of biochar produced by pyrolysis are lower compared with those of the original raw biomass. Furthermore, marked drops in H/C and O/C molar ratios were observed with increasing pyrolysis temperature, thus highlighting a higher degree of carbonization and char stability.

The European Biochar Certificate (EBC) guidelines recommend upper limits for molar H/C<sub>org</sub> and O/C<sub>org</sub> ratios in





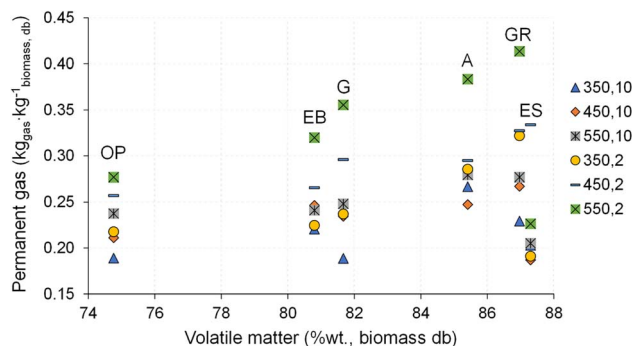


Fig. 16 Influence of VM content of biomass on the yield of permanent gas.

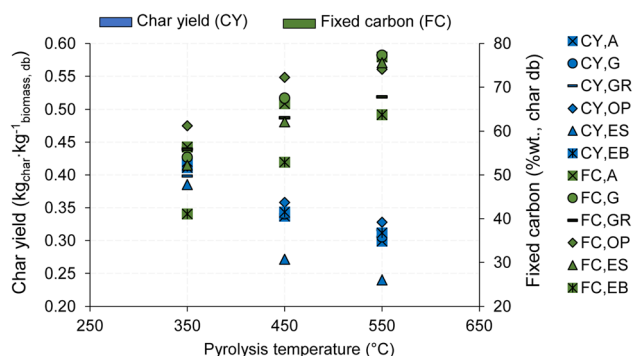


Fig. 17 Influence of pyrolysis temperature on biochar yield and FC content during the pyrolysis of different biomass types at 10 °C min<sup>-1</sup> (heating rate).

biochar, which are 0.7 and 0.4, respectively, and higher values may indicate non-pyrolytic chars.<sup>42</sup> As mentioned in section 3.1, these guidelines do not include the inorganic carbon in biochar. However, in line with the literature for similar biomass types to those analyzed in this study, the calcium concentration in biochar is exceedingly low, and the inorganic carbon in the char is primarily in the form of carbonates, typically as calcite, thus rendering its presence minimal and insignificant compared to the substantial total carbon content of the biochar. Thus, in this study, the H/C and O/C molar ratios were

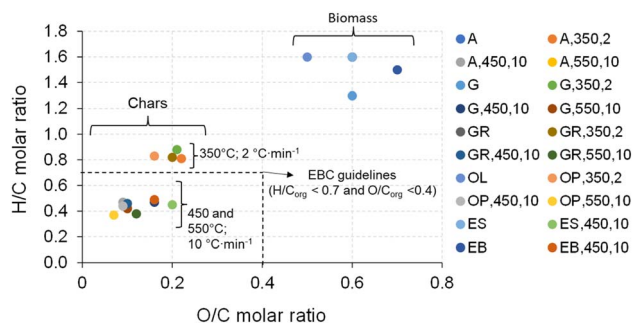


Fig. 18 Van Krevelen diagram of biochar produced at different pyrolysis temperatures and heating rates in comparison with the respective biomass.

determined considering the total carbon, and then compared with the EBC guidelines.

Overall, the H/C and O/C molar ratios of biochars produced from all biomass types are relatively lower than the values indicated by the EBC guidelines, with the exception of the biochars produced at 350 °C and 2 °C min<sup>-1</sup>, which fall outside (with values between 0.81 and 0.88) the indicated EBC H/C<sub>org</sub> limits. The results observed for biochars produced at 450 °C and 10 °C min<sup>-1</sup> and 550 °C and 10 °C min<sup>-1</sup> indicate a high stability of the biochar and a high degree of carbonization.

## 4. Summary of the results and comparison to the literature

Throughout this study, detailed analyses were conducted on the results obtained under the established operating conditions in a bench-scale fixed bed reactor. These analyses allowed for a comprehensive comparison with data available in the literature from studies conducted under similar operational conditions (Table 3).

In general, the results achieved in this work are in line with the data found in the literature. However, there are some noteworthy variations that deserve highlighting. Regarding product yields, it is observed that the maximum biochar yield in this study is slightly higher, while the minimum bio-oil yield is slightly lower compared to those in the literature. Concerning biochar composition, the maximum volatile matter content in the biochar exceeds the values found in the literature. Additionally, the minimum fixed carbon content in the biochar is lower than the reference data. These differences can be attributed to specific operational variables, such as lower heating rates, and the characteristics of the biomasses used.

In addition to the comparison with literature data under similar conditions, Table 3 allows for a comparison of the results obtained in the fixed bed with other pyrolysis technologies. It is observed that the fixed bed reactor demonstrates a tendency to produce higher biochar yields and lower bio-oil yields compared to other technologies, such as fluidized bed and spouted bed reactors. This aligns with the literature.<sup>7</sup> These technologies have distinct hydrodynamic behaviors and, therefore, different operational patterns, such as the gas-solid contact model, heating rates, and residence times.<sup>58</sup> Fluidized beds and spouted bed reactors allow for higher heating rates of biomass particles and shorter gas residence times, favoring the formation of condensable vapors (bio-oil).

Furthermore, it is noted that the spouted bed reactor stands out for producing the highest bio-oil yields, making it a viable alternative for obtaining this specific product. Spouted bed reactors represent an alternative to fluidized bed reactors for the fast pyrolysis of biomass. They facilitate high rates of heat and mass transfer, as well as efficient particle movement, allowing for even shorter gas residence times than fluidized bed reactors (in milliseconds),<sup>59</sup> thereby reducing secondary reactions.

Based on the experimental results obtained in this study, it is evident that the yield and characteristics of the biochar, bio-oil and permanent gas produced during the pyrolysis of residual



Table 3 Comparison of the results obtained in the fixed bed reactor with other pyrolysis technologies

|                                  | This work                             | Fixed bed reactor <sup>12,14,20,60–62</sup> | Fluidized bed reactor <sup>63–66</sup> | Spouted bed reactor <sup>67,68</sup> |
|----------------------------------|---------------------------------------|---|--|--------------------------------------|
| Operating conditions             | 350–550 °C; 2–30 °C min <sup>−1</sup> | 300–650 °C; 3–30 °C min <sup>−1</sup>       | 400–500 °C                             | 400–500 °C                           |
| <b>Biomass composition</b>       |                                       |   |  |                                      |
| VM (%wt., db)                    | 74.8–87.3                             | 66.8–92.3                                   | 78.6–78.7                              | —                                    |
| FC (%wt., db)                    | 9.4–19.8                              | 7.6–22.6                                    | 14.8–18.8                              | —                                    |
| Ash (%wt., db)                   | 0.8–5.4                               | 0.4–10.8                                    | 0.3–2.6                                | —                                    |
| <b>Product yield</b>             |                                       |   |  |                                      |
| Biochar                          | 0.22–0.47                             | 0.22–0.40                                   | 0.13–0.21                              | 0.18–0.22                            |
| Bio-oil                          | 0.26–0.59                             | 0.39–0.60                                   | 0.57–0.69                              | 0.71–0.75                            |
| Permanent gas                    | 0.17–0.41                             | 0.16–0.36                                   | 0.11–0.26                              | 0.06                                 |
| <b>Biochar composition</b>       |                                       |   |  |                                      |
| VM (%wt., db)                    | 12.4–58.1                             | 6.7–35.1                                    | —                                      | 37.6                                 |
| FC (%wt., db)                    | 38.0–77.3                             | 49.4–88.9                                   | —                                      | 60.2                                 |
| Ash (%wt., db)                   | 1.11–13.19                            | 1.1–30.3                                    | —                                      | 2.2                                  |
| C (%wt., daf)                    | 72.6–88.3                             | 70.0–95.2                                   | 90.0                                   | 73.3                                 |
| H (%wt., daf)                    | 2.7–5.3                               | 1.5–3.6                                     | 1.4                                    | 3.7                                  |
| N (%wt., daf)                    | 0.4–1.8                               | 0.6–8.3                                     | —                                      | 0.2                                  |
| O (%wt., daf)                    | 7.8–20.9                              | 0.6–22.6                                    | —                                      | 20.6                                 |
| LHV (MJ Nm <sup>−3</sup> )       | 24.2–30.5                             | 21.4–34.9                                   | 32.2                                   | 21.6                                 |
| <b>Permanent gas composition</b> |                                       |   |  |                                      |
| CO (%v)                          | 27.7–36.9                             | —   | 42.0–46.0                              | 41.7                                 |
| CO <sub>2</sub> (%v)             | 44.3–61.1                             | —   | 44.0–50.4                              | 33.7                                 |
| CH <sub>4</sub> (%v)             | 2.5–11.8                              | —   | 4.8–6.5                                | 9.3                                  |
| H <sub>2</sub> (%v)              | 0.6–6.9                               | —   | 0.10–2.2                               | 10.6                                 |
| LHV (MJ Nm <sup>−3</sup> )       | 5.4–9.7                               | —   | —                                      | —                                    |

biomass can vary significantly, depending on the biomass type, process temperature, heating rate and technology. This variability must be taken into account and thoroughly evaluated to effectively support the development and scale-up of pyrolysis for each specific product and its application.

## 5. Conclusions

In this study, pyrolysis of residual forestry and agroforestry biomass was studied in a bench-scale reactor, focusing on the impact of pyrolysis temperature, heating rate and biomass characteristics on the distribution and composition of biochar, bio-oil and permanent gases.

For the experimental conditions tested (temperatures in the range of 350 to 550 °C, and heating rates from 2 to 30 °C min<sup>−1</sup>), biochar, bio-oil and permanent gas yields ranged from 0.22 to 0.47, 0.26 to 0.59, and 0.17 to 0.41 kg kg<sup>−1</sup> dry biomass, respectively. Olive pomace pyrolysis had the higher biochar yield, eucalyptus sawdust pyrolysis had the higher bio-oil yield, and giant reed pyrolysis had the higher permanent gas yield.

In relation to the effect of the pyrolysis temperature and heating rate on the biochar yield and composition, an increase in temperature and heating rate resulted in a decrease in biochar yield, a decrease in volatile matter content, an increase in fixed carbon content, an increase in ash content, and a decrease in the H/C and O/C molar ratios in biochar. However, the effect of the heating rate appears to have less impact than that of

temperature. The biochar produced at 450 °C and 10 °C min<sup>−1</sup> and 550 °C and 10 °C min<sup>−1</sup> meets EBC guidelines for carbon content and H/C and O/C molar ratios, and has the potential to be used as biochar for soil application. Furthermore, it was observed that this biochar has the potential to enrich the soil with nutrients due to the increased inorganic content in the material while also showing promise for carbon sequestration. Additionally, the LHV of biochar was between 24.2 and 30.5 MJ kg<sup>−1</sup> dry biochar, indicating its potential as an energy vector, despite the high ash content that may pose challenges in certain applications.

Regarding bio-oil, an increase in the temperature and heating rate led to an increase in bio-oil yield.

Concerning permanent gas composition, an increase in pyrolysis temperature promotes an improvement in the permanent gas quality, because it caused a decrease in CO<sub>2</sub>, an increase in CH<sub>4</sub> and H<sub>2</sub> concentration, and, consequently, an increase in the LHV. The higher LHV value was 9.7 MJ Nm<sup>−3</sup>, which is interesting for use as a thermal energy source to support the pyrolysis process.

With respect to the effect of FC and VM of raw biomass on pyrolysis products, it is observed that higher FC content in biomass led to higher char yield at the lowest temperature (350 °C), but no significant trends were observed for the higher temperatures (450 and 550 °C), especially for similar FC contents of the biomass. Higher VM content in biomass appeared to lead to higher permanent gas yield, except for eucalyptus sawdust pyrolysis.



This study provides valuable information to support the development and scale-up of pyrolysis technology for the conversion of various types of residual biomass into valuable bioproducts. Further research is needed to analyze the influence of the operating conditions on the bio-oil composition.

## Abbreviations

|                            |  |
|----------------------------|--|
| A                          | Acacia   |
| db                         | Dry basis  |
| daf                        | Dry ash free   |
| EB                         | Eucalyptus bark  |
| ES                         | Eucalyptus sawdust   |
| FC                         | Fixed carbon   |
| G                          | Gorse  |
| GR                         | Giant reed   |
| LHV                        | Lower heating value  |
| $m_{\text{bm,wb}}$         | Mass of biomass (wet basis) loaded in the reactor, kg  |
| $m_{\text{bm,db}}$         | Mass of biomass (dry basis) loaded in the reactor, kg  |
| $m_{\text{bio-oil}}$       | Mass of condensed bio-oil, kg  |
| $m_{\text{biochar}}$       | Mass of biochar, kg  |
| $m_{\text{gas}}$           | Mass of permanent gas, kg  |
| $\eta_{\text{biochar,db}}$ | Yield of biochar, ratio between mass of biochar and mass of biomass on a dry basis, $\text{kg}_{\text{biochar}} \text{kg}_{\text{biomass dry basis}}^{-1}$         |
| $\eta_{\text{boil,db}}$    | Yield of bio-oil, ratio between mass of bio-oil and mass of biomass on a dry basis, $\text{kg}_{\text{bio-oil}} \text{kg}_{\text{biomass dry basis}}^{-1}$         |
| $\eta_{\text{gas,db}}$     | Yield of permanent gas, ratio between mass of permanent gas and mass of biomass on a dry basis, $\text{kg}_{\text{gas}} \text{kg}_{\text{biomass dry basis}}^{-1}$ |
| NPT                        | Standard pressure ( $1.013 \times 10^5$ Pa) and temperature (273 K)  |
| $\text{Nm}^3$              | $\text{m}^3$ referred at standard pressure ( $1.013 \times 10^5$ Pa) and temperature (273 K)   |
| OP                         | Olive pomace   |
| wb                         | Wet basis  |
| $w_{\text{i,bm}}$          | Mass fraction of $i$ chemical element, CHNSO, in biomass, $\text{kg i kg}^{-1} \text{bm, db}$  |
| $w_{\text{i,bio-oil}}$     | Mass fraction of $i$ chemical element, CHNSO, in bio-oil, $\text{kg i kg}^{-1} \text{bm, db}$  |
| $w_{\text{i,biochar}}$     | Mass fraction of $i$ chemical element, CHNSO, in biochar, $\text{kg i kg}^{-1} \text{bm, db}$  |
| $w_{\text{i,gas}}$         | Mass fraction of $i$ chemical element, CHNSO, in permanent gas, $\text{kg i kg}^{-1} \text{bm, db}$  |
| VM                         | Volatile matter  |

## Conflicts of interest

There are no conflicts to declare.

## Acknowledgements

This work was carried out under Project BioValChar – Sustainable valorisation of residual biomass for biochar, PCIF-GVB-0034-2019, funded by the Portuguese Foundation for Science and Technology (FCT), and Project INPACTUS – innovative

products and technologies from eucalyptus, Project No. 21874 funded by Portugal 2020 through the European Regional Development Fund (ERDF) in the frame of COMPETE 2020 no. 246/AXIS II/2017. Thanks are due to the Portuguese Foundation for Science and Technology (FCT)/Ministry of Science, Technology and Higher Education (MCTES), Portugal, for the financial support to CESAM (UIDP/50017/2020+UIDB/50017/2020+LA/P/0094/2020), through national funds. Thanks are also due to the FCT/MCTES for providing financial support to the PhD scholarship granted to A. C. M. Vilas-Boas (ref. 2021.08162.BD).

## References

- 1 D. Gielen, D. Saygin, A. Lopez-Peña, N. Wagner, G. Prakash, S. Teske, *et al.*, *Methodology Background Document: Development of a Decarbonisation Pathway for the Global Energy System to 2050. A Country-By-Country Analysis for the G20 Based on IRENA's REmap and Renewable Energy Benefits Programmes*, Irena, 2020.
- 2 G. Wang, B. Fan, H. Chen and Y. Li, Understanding the pyrolysis behavior of agriculture, forest and aquatic biomass: Products distribution and characterization, *J. Energy Inst.*, 2020, **93**, 1892–1900, DOI: [10.1016/j.joei.2020.04.004](https://doi.org/10.1016/j.joei.2020.04.004).
- 3 S. Wang, G. Dai, H. Yang and Z. Luo, Lignocellulosic biomass pyrolysis mechanism: A state-of-the-art review, *Prog. Energy Combust. Sci.*, 2017, **62**, 33–86, DOI: [10.1016/j.pecs.2017.05.004](https://doi.org/10.1016/j.pecs.2017.05.004).
- 4 S. Papari and K. Hawboldt, A review on the pyrolysis of woody biomass to bio-oil: Focus on kinetic models, *Renewable Sustainable Energy Rev.*, 2015, **52**, 1580–1595, DOI: [10.1016/j.rser.2015.07.191](https://doi.org/10.1016/j.rser.2015.07.191).
- 5 F. Ronsse, R. W. Nachenius and W. Prins, Carbonization of Biomass, *Recent Advances in Thermochemical Conversion of Biomass*, Elsevier B.V., 2015, Ch. 11, DOI: [10.1016/B978-0-444-63289-0.00011-9](https://doi.org/10.1016/B978-0-444-63289-0.00011-9).
- 6 P. Roy and G. Dias, Prospects for pyrolysis technologies in the bioenergy sector: A review, *Renewable Sustainable Energy Rev.*, 2017, **77**, 59–69, DOI: [10.1016/j.rser.2017.03.136](https://doi.org/10.1016/j.rser.2017.03.136).
- 7 P. Basu, *Biomass Gasification and Pyrolysis: Practical Design*, 2010.
- 8 D. Neves, H. Thunman, A. Matos, L. Tarelho and A. Gómez-Barea, Characterization and prediction of biomass pyrolysis products, *Prog. Energy Combust. Sci.*, 2011, **37**, 611–630, DOI: [10.1016/j.pecs.2011.01.001](https://doi.org/10.1016/j.pecs.2011.01.001).
- 9 L. Zhang, C. C. Xu and P. Champagne, Overview of recent advances in thermo-chemical conversion of biomass, *Energy Convers. Manage.*, 2010, **51**, 969–982, DOI: [10.1016/j.enconman.2009.11.038](https://doi.org/10.1016/j.enconman.2009.11.038).
- 10 M. Van de Velden, J. Baeyens, A. Brems, B. Janssens and R. Dewil, Fundamentals, kinetics and endothermicity of the biomass pyrolysis reaction, *Renewable Energy*, 2010, **35**, 232–242, DOI: [10.1016/j.renene.2009.04.019](https://doi.org/10.1016/j.renene.2009.04.019).
- 11 A. Tuan, H. Chyuan, I. M. R. Fattah, C. Tung, C. Kui, R. Sakthivel, *et al.*, Progress on the lignocellulosic biomass pyrolysis for biofuel production toward environmental



- sustainability, *Fuel Process. Technol.*, 2021, **223**, 106997, DOI: [10.1016/j.fuproc.2021.106997](https://doi.org/10.1016/j.fuproc.2021.106997).
- 12 E. Apaydin-Varol and A. E. Pütün, Preparation and characterization of pyrolytic chars from different biomass samples, *J. Anal. Appl. Pyrolysis*, 2012, **98**, 29–36, DOI: [10.1016/j.jaap.2012.07.001](https://doi.org/10.1016/j.jaap.2012.07.001).
  - 13 N. Gómez, J. G. Rosas, J. Cara, O. Martínez, J. A. Albuquerque and M. E. Sánchez, Slow pyrolysis of relevant biomasses in the Mediterranean basin. Part 1. Effect of temperature on process performance on a pilot scale, *J. Cleaner Prod.*, 2016, **120**, 181–190, DOI: [10.1016/j.jclepro.2014.10.082](https://doi.org/10.1016/j.jclepro.2014.10.082).
  - 14 F. A. López, T. A. Centeno, I. García-Díaz and F. J. Alguacil, Textural and fuel characteristics of the chars produced by the pyrolysis of waste wood, and the properties of activated carbons prepared from them, *J. Anal. Appl. Pyrolysis*, 2013, **104**, 551–558, DOI: [10.1016/j.jaap.2013.05.014](https://doi.org/10.1016/j.jaap.2013.05.014).
  - 15 M. Tripathi, J. N. Sahu and P. Ganesan, Effect of process parameters on production of biochar from biomass waste through pyrolysis: A review, *Renewable Sustainable Energy Rev.*, 2016, **55**, 467–481, DOI: [10.1016/j.rser.2015.10.122](https://doi.org/10.1016/j.rser.2015.10.122).
  - 16 J. Parikh, S. A. Channiwala and G. K. Ghosal, A correlation for calculating HHV from proximate analysis of solid fuels, *Fuel*, 2005, **84**, 487–494, DOI: [10.1016/j.fuel.2004.10.010](https://doi.org/10.1016/j.fuel.2004.10.010).
  - 17 V. Dhyani and T. Bhaskar, A comprehensive review on the pyrolysis of lignocellulosic biomass, *Renewable Energy*, 2018, **129**, 695–716, DOI: [10.1016/j.renene.2017.04.035](https://doi.org/10.1016/j.renene.2017.04.035).
  - 18 J. Y. Park, J. K. Kim, C. H. Oh, J. W. Park and E. E. Kwon, Production of bio-oil from fast pyrolysis of biomass using a pilot-scale circulating fluidized bed reactor and its characterization, *J. Environ. Manage.*, 2019, **234**, 138–144, DOI: [10.1016/j.jenvman.2018.12.104](https://doi.org/10.1016/j.jenvman.2018.12.104).
  - 19 M. Pala, P. S. Marathe, X. Hu, F. Ronsse, W. Prins, S. R. A. Kersten, *et al.*, Recycling of product gas does not affect fast pyrolysis oil yield and composition, *J. Anal. Appl. Pyrolysis*, 2020, **148**, 104794, DOI: [10.1016/j.jaap.2020.104794](https://doi.org/10.1016/j.jaap.2020.104794).
  - 20 T. Aysu and M. M. Küçük, Biomass pyrolysis in a fixed-bed reactor: Effects of pyrolysis parameters on product yields and characterization of products, *Energy*, 2014, **64**, 1002–1025, DOI: [10.1016/j.energy.2013.11.053](https://doi.org/10.1016/j.energy.2013.11.053).
  - 21 C. E. Efika, J. A. Onwudili and P. T. Williams, Influence of heating rates on the products of high-temperature pyrolysis of waste wood pellets and biomass model compounds, *Waste Manage.*, 2018, **76**, 497–506, DOI: [10.1016/j.wasman.2018.03.021](https://doi.org/10.1016/j.wasman.2018.03.021).
  - 22 S. Czernik and A. V. Bridgwater, Overview of applications of biomass fast pyrolysis oil, *Energy Fuels*, 2004, **18**, 590–598, DOI: [10.1021/ef034067u](https://doi.org/10.1021/ef034067u).
  - 23 A. V. Bridgwater, Review of fast pyrolysis of biomass and product upgrading, *Biomass Bioenergy*, 2012, **38**, 68–94, DOI: [10.1016/j.biombioe.2011.01.048](https://doi.org/10.1016/j.biombioe.2011.01.048).
  - 24 F. Ronsse, S. van Hecke, D. Dickinson and W. Prins, Production and characterization of slow pyrolysis biochar: Influence of feedstock type and pyrolysis conditions, *GCB Bioenergy*, 2013, **5**, 104–115, DOI: [10.1111/gcbb.12018](https://doi.org/10.1111/gcbb.12018).
  - 25 T. Kiuru and J. Hyytiäinen, *Review of Current Biocoal Production Technology*, *Balt Bioenergy Ind Charcoal*, 2013, **4**.
  - 26 J. Liang, Y. Li, B. Si, Y. Wang, X. Chen, X. Wang, *et al.*, Optimizing biochar application to improve soil physical and hydraulic properties in saline-alkali soils, *Sci. Total Environ.*, 2021, **771**, DOI: [10.1016/j.scitotenv.2020.144802](https://doi.org/10.1016/j.scitotenv.2020.144802).
  - 27 A. C. M. Vilas-boas, L. A. C. Tarelho, M. Kamali, D. T. Pio, D. Jahanianfard and A. P. D. Gomes, Biochar from Slow Pyrolysis of Biological Sludge from Wastewater Treatment: Characteristics and Effect as Soil Amendment, *Biofuels Bioprod. Bioref.*, 2021, **15**, 1054–1072, DOI: [10.1002/bbb.2220](https://doi.org/10.1002/bbb.2220).
  - 28 J. S. Cha, S. H. Park, S. C. Jung, C. Ryu, J. K. Jeon, M. C. Shin, *et al.*, Production and utilization of biochar: A review, *J. Ind. Eng. Chem.*, 2016, **40**, 1–15, DOI: [10.1016/j.jiec.2016.06.002](https://doi.org/10.1016/j.jiec.2016.06.002).
  - 29 S. I. Yang, T. C. Hsu, C. Y. Wu, K. H. Chen, Y. L. Hsu and Y. H. Li, Application of biomass fast pyrolysis part II: The effects that bio-pyrolysis oil has on the performance of diesel engines., *Energy*, 2014, **66**, 172–180, DOI: [10.1016/j.energy.2013.12.057](https://doi.org/10.1016/j.energy.2013.12.057).
  - 30 X. Zhou, T. B. Moghaddam, M. Chen, S. Wu, Y. Zhang, X. Zhang, *et al.*, Effects of pyrolysis parameters on physicochemical properties of biochar and bio-oil and application in asphalt, *Sci. Total Environ.*, 2021, **780**, 146448, DOI: [10.1016/j.scitotenv.2021.146448](https://doi.org/10.1016/j.scitotenv.2021.146448).
  - 31 C. T. Primaz, T. Schena, E. Lazzari, E. B. Caramão and R. A. Jacques, Influence of the temperature in the yield and composition of the bio-oil from the pyrolysis of spent coffee grounds: Characterization by comprehensive two dimensional gas chromatography, *Fuel*, 2018, **232**, 572–580, DOI: [10.1016/j.fuel.2018.05.097](https://doi.org/10.1016/j.fuel.2018.05.097).
  - 32 R. O. Farias, P. Vanessa, S. Lins, R. Gabriel, A. David, R. Silva, *et al.*, Pyrolysis of Coconut Inflorescence Wastes: Production, Effects of Parameters, Characterization and Optimization of Phenolic - Rich Bio - Oil, *Int. J. Environ. Res.*, 2022, **16**, 15, DOI: [10.1007/s41742-022-00393-x](https://doi.org/10.1007/s41742-022-00393-x).
  - 33 C. Setter, F. T. M. Silva, M. R. Assis, C. H. Ataíde, P. F. Trugilho and T. J. P. Oliveira, Slow pyrolysis of coffee husk briquettes: Characterization of the solid and liquid fractions, *Fuel*, 2020, **261**, 116420, DOI: [10.1016/j.fuel.2019.116420](https://doi.org/10.1016/j.fuel.2019.116420).
  - 34 A. Zhao, S. Liu, J. Yao, F. Huang, Z. He and J. Liu, Characteristics of bio-oil and biochar from cotton stalk pyrolysis: Effects of torrefaction temperature and duration in an ammonia environment, *Bioresour. Technol.*, 2022, **343**, 126145, DOI: [10.1016/j.biortech.2021.126145](https://doi.org/10.1016/j.biortech.2021.126145).
  - 35 V. Dhyani and T. Bhaskar, A comprehensive review on the pyrolysis of lignocellulosic biomass, *Renewable Energy*, 2018, **129**, 695–716, DOI: [10.1016/j.renene.2017.04.035](https://doi.org/10.1016/j.renene.2017.04.035).
  - 36 M. Afraz, F. Muhammad, J. Nisar, A. Shah, S. Munir, G. Ali, *et al.*, Production of value added products from biomass waste by pyrolysis: An updated review, *Waste Manag. Bull.*, 2024, **1**, 30–40, DOI: [10.1016/j.wmb.2023.08.004](https://doi.org/10.1016/j.wmb.2023.08.004).
  - 37 M. Ortiz, *Biomass Pyrolysis Dataset*, 2021, DOI: [10.17632/bx88ymgbbv.1](https://doi.org/10.17632/bx88ymgbbv.1).
  - 38 D. O. Usino, Supriyanto, P. Ylittervo, A. Pettersson and T. Richards, Influence of temperature and time on initial





- pyrolysis of cellulose and xylan, *J. Anal. Appl. Pyrolysis*, 2020, **147**, 104782, DOI: [10.1016/j.jaap.2020.104782](https://doi.org/10.1016/j.jaap.2020.104782).
- 39 G. Dorez, L. Ferry, R. Sonnier, A. Taguet and J. M. Lopez-Cuesta, Effect of cellulose, hemicellulose and lignin contents on pyrolysis and combustion of natural fibers, *J. Anal. Appl. Pyrolysis*, 2014, **107**, 323–331, DOI: [10.1016/j.jaap.2014.03.017](https://doi.org/10.1016/j.jaap.2014.03.017).
  - 40 R. E. Guedes, A. S. Luna and A. R. Torres, Operating parameters for bio-oil production in biomass pyrolysis: A review, *J. Anal. Appl. Pyrolysis*, 2018, **129**, 134–149, DOI: [10.1016/j.jaap.2017.11.019](https://doi.org/10.1016/j.jaap.2017.11.019).
  - 41 A. Tomczyk, Z. Sokołowska and P. Boguta, Biochar physicochemical properties: pyrolysis temperature and feedstock kind effects, *Rev. Environ. Sci. Biotechnol.*, 2020, **19**, 191–215, DOI: [10.1007/s11157-020-09523-3](https://doi.org/10.1007/s11157-020-09523-3).
  - 42 European Biochar Foundation (EBC), *Guidelines for a Sustainable Production of Biochar*. Eur Biochar Found., 2021, pp. 1–22.
  - 43 A. Budai, A. R. Zimmerman, A. L. Cowie, J. B. W. Webber, B. P. Singh, B. Glaser, *et al.*, Biochar Carbon Stability Test Method : An assessment of methods to determine biochar carbon stability, *Int Biochar Initiat.*, 2013, 1–10.
  - 44 D. T. Pio, L. A. C. Tarelho, T. F. V. Nunes, M. F. Baptista and M. A. A. Matos, Co-combustion of residual forest biomass and sludge in a pilot-scale bubbling fluidized bed, *J. Cleaner Prod.*, 2020, **249**, 119309, DOI: [10.1016/j.jclepro.2019.119309](https://doi.org/10.1016/j.jclepro.2019.119309).
  - 45 T. Kan, V. Strezov and T. J. Evans, Lignocellulosic biomass pyrolysis: A review of product properties and effects of pyrolysis parameters, *Renewable Sustainable Energy Rev.*, 2016, **57**, 1126–1140, DOI: [10.1016/j.rser.2015.12.185](https://doi.org/10.1016/j.rser.2015.12.185).
  - 46 A. Björkman, Projects on coal characterization, *Fuel*, 2001, **80**, 155–166, DOI: [10.1016/S0016-2361\(00\)00090-9](https://doi.org/10.1016/S0016-2361(00)00090-9).
  - 47 B. Khiari, M. Jeguirim, L. Limousy and S. Bennici, Biomass derived chars for energy applications, *Renewable Sustainable Energy Rev.*, 2019, **108**, 253–273, DOI: [10.1016/j.rser.2019.03.057](https://doi.org/10.1016/j.rser.2019.03.057).
  - 48 A. Zulkania, G. F. Hanum and A. Sri Rezki, The potential of activated carbon derived from bio-char waste of bio-oil pyrolysis as adsorbent, *MATEC Web Conf.*, 2018, **154**, 1–6, DOI: [10.1051/mateconf/201815401029](https://doi.org/10.1051/mateconf/201815401029).
  - 49 F. Abnisa, A. Arami-Niya, W. M. A. Wan Daud, J. N. Sahu and I. M. Noor, Utilization of oil palm tree residues to produce bio-oil and bio-char via pyrolysis, *Energy Convers. Manage.*, 2013, **76**, 1073–1082, DOI: [10.1016/j.enconman.2013.08.038](https://doi.org/10.1016/j.enconman.2013.08.038).
  - 50 G. Kumar, A. K. Panda and R. K. Singh, Optimization of process for the production of bio-oil from eucalyptus wood, *J. Fuel Chem. Technol.*, 2010, **38**, 162–167, DOI: [10.1016/S1872-5813\(10\)60028-X](https://doi.org/10.1016/S1872-5813(10)60028-X).
  - 51 N. Ahmed, M. Zeeshan, N. Iqbal and M. Zohaib, Investigation on bio-oil yield and quality with scrap tire addition in sugarcane bagasse pyrolysis, *J. Cleaner Prod.*, 2018, **196**, 927–934, DOI: [10.1016/j.jclepro.2018.06.142](https://doi.org/10.1016/j.jclepro.2018.06.142).
  - 52 A. Sharma, V. Pareek and D. Zhang, Biomass pyrolysis - A review of modelling, process parameters and catalytic studies, *Renewable Sustainable Energy Rev.*, 2015, **50**, 1081–1096, DOI: [10.1016/j.rser.2015.04.193](https://doi.org/10.1016/j.rser.2015.04.193).
  - 53 G. Ø. Flatabø, G. Cornelissen, P. Carlsson, P. J. Nilsen, D. Tapasvi, W. H. Bergland, *et al.*, Industrially relevant pyrolysis of diverse contaminated organic wastes: Gas compositions and emissions to air, *J. Cleaner Prod.*, 2023, **423**, DOI: [10.1016/j.jclepro.2023.138777](https://doi.org/10.1016/j.jclepro.2023.138777).
  - 54 S. Honus, D. Juchelkova, A. Campen and T. Wiltowski, Gaseous components from pyrolysis - Characteristics, production and potential for energy utilization, *J. Anal. Appl. Pyrolysis*, 2014, **106**, 1–8, DOI: [10.1016/j.jaap.2013.11.023](https://doi.org/10.1016/j.jaap.2013.11.023).
  - 55 F. Charvet, F. Silva, D. Pio, L. Tarelho, A. Matos, J. Silva, *et al.*, Charcoal production from alternative agroforestry woody residues typical of southern europe, *Eur. Biomass Conf. Exhib.*, 2020, 368–376.
  - 56 J. A. Alburquerque, M. E. Sánchez, M. Mora and V. Barrón, Slow pyrolysis of relevant biomasses in the Mediterranean basin. Part 2. Char characterisation for carbon sequestration and agricultural uses, *J. Cleaner Prod.*, 2016, **120**, 191–197, DOI: [10.1016/j.jclepro.2014.10.080](https://doi.org/10.1016/j.jclepro.2014.10.080).
  - 57 F. R. Oliveira, A. K. Patel, D. P. Jaisi, S. Adhikari, H. Lu and S. K. Khanal, Environmental application of biochar: Current status and perspectives, *Bioresour. Technol.*, 2017, **246**, 110–122, DOI: [10.1016/j.biortech.2017.08.122](https://doi.org/10.1016/j.biortech.2017.08.122).
  - 58 D. T. Pio, L. A. C. Tarelho and M. A. A. Matos, Characteristics of the gas produced during biomass direct gasification in an autothermal pilot-scale bubbling fluidized bed reactor, *Energy*, 2017, **120**, 915–928, DOI: [10.1016/j.energy.2016.11.145](https://doi.org/10.1016/j.energy.2016.11.145).
  - 59 H. C. Park and H. S. Choi, Fast pyrolysis of biomass in a spouted bed reactor: Hydrodynamics, heat transfer and chemical reaction, *Renewable Energy*, 2019, **143**, 1268–1284, DOI: [10.1016/j.renene.2019.05.072](https://doi.org/10.1016/j.renene.2019.05.072).
  - 60 Y. Lee, J. Park, C. Ryu, K. S. Gang, W. Yang, Y. K. Park, *et al.*, Comparison of biochar properties from biomass residues produced by slow pyrolysis at 500°C, *Bioresour. Technol.*, 2013, **148**, 196–201, DOI: [10.1016/j.biortech.2013.08.135](https://doi.org/10.1016/j.biortech.2013.08.135).
  - 61 S. G. C. de Almeida, L. A. C. Tarelho, T. Hauschild, M. A. M. Costa and K. J. Dussán, Biochar production from sugarcane biomass using slow pyrolysis: Characterization of the solid fraction, *Chem. Eng. Process.*, 2022, **179**, 109054, DOI: [10.1016/j.ccep.2022.109054](https://doi.org/10.1016/j.ccep.2022.109054).
  - 62 A. K. S. Pereira, D. L. Júnior, Á. M. da Silva, E. C. de Souza, F. M. Delatorre, B. P. Rodrigues and A. F. D. Júnior, Understanding the Impacts of Pyrolysis Temperature on the Energy Performance of Eucalyptus spp. Charcoal, *Environ. Sci. Proc.*, 2022, **13**, 25, DOI: [10.3390/iescf2021-10794](https://doi.org/10.3390/iescf2021-10794).
  - 63 J. E. Joubert, M. Carrier, N. Dahmen, R. Stahl and J. H. Knoetze, Inherent process variations between fast pyrolysis technologies: A case study on Eucalyptus grandis, *Fuel Process. Technol.*, 2015, **131**, 389–395, DOI: [10.1016/j.fuproc.2014.12.012](https://doi.org/10.1016/j.fuproc.2014.12.012).
  - 64 K. H. Kim, T. S. Kim, S. M. Lee, D. Choi, H. Yeo, I. G. Choi, *et al.*, Comparison of physicochemical features of biooils and biochars produced from various woody biomasses by fast pyrolysis, *Renewable Energy*, 2013, **50**, 188–195, DOI: [10.1016/j.renene.2012.06.030](https://doi.org/10.1016/j.renene.2012.06.030).
  - 65 H. Zhang, R. Xiao, D. Wang, G. He, S. Shao, J. Zhang, *et al.*, Biomass fast pyrolysis in a fluidized bed reactor under N<sub>2</sub>,



- CO<sub>2</sub>, CO, CH<sub>4</sub> and H<sub>2</sub> atmospheres, *Bioresour. Technol.*, 2011, **102**, 4258–4264, DOI: [10.1016/j.biortech.2010.12.075](https://doi.org/10.1016/j.biortech.2010.12.075).
- 66 Q. K. Tran, M. L. Le, H. V. Ly, H. C. Woo, J. Kim and S. S. Kim, Fast pyrolysis of pitch pine biomass in a bubbling fluidized-bed reactor for bio-oil production, *J. Ind. Eng. Chem.*, 2021, **98**, 168–179, DOI: [10.1016/j.jiec.2021.04.005](https://doi.org/10.1016/j.jiec.2021.04.005).
- 67 M. Amutio, G. Lopez, M. Artetxe, G. Elordi, M. Olazar and J. Bilbao, Influence of temperature on biomass pyrolysis in a conical spouted bed reactor, *Resour., Conserv. Recycl.*, 2012, **59**, 23–31, DOI: [10.1016/j.resconrec.2011.04.002](https://doi.org/10.1016/j.resconrec.2011.04.002).
- 68 M. Amutio, G. Lopez, J. Alvarez, M. Olazar and J. Bilbao, Fast pyrolysis of eucalyptus waste in a conical spouted bed reactor, *Bioresour. Technol.*, 2015, **194**, 225–232, DOI: [10.1016/j.biortech.2015.07.030](https://doi.org/10.1016/j.biortech.2015.07.030).

